Non-linear dynamic and static analyses on eight historical masonry towers in the North-East of Italy

Marco Valente, Gabriele Milani *

Department of Architecture, Built Environment and Construction Engineering, Politecnico di Milano, Piazza Leonardo da Vinci 32, 20133 Milano, Italy

The behavior of eight historical masonry towers, located in the North-East region of Italy, is analyzed under horizontal loads by means of detailed 3D FE models. The geometry of the towers is deduced from both existing available documentation and in-situ surveys. The towers, albeit unique for geometric and architectural features, show some affinities that justify a comparative analysis, as for instance the location and the similar masonry material. Their structural behavior under horizontal loads is therefore influenced by geometrical issues, such as slenderness, walls thickness, openings, presence of internal vaults and irregularities.

Non-linear dynamic analyses are performed on detailed 3D FE models of the towers using a real accelerogram with different peak ground accelerations. A damage plasticity material model, exhibiting softening in both tension and compression, is used for masonry. Non-linear dynamic simulations show the high vulnerability of ancient masonry towers under horizontal loads. Numerical results are then compared with a non-linear static procedure based on pushover analyses in terms of displacement demand and tensile damage distribution. It is found that the results obtained with the non-linear static procedure are in a good agreement with those obtained through more time-consuming non-linear dynamic simulations, with a slight less conservative trend.

Keywords: Masonry towers, 3D FE models, Non-linear dynamic analysis, Non-linear static procedure

1. Introduction

The protection of historical masonry constructions against seismic actions is of strategic importance in many European countries, especially in Italy, which are prone to earthquakes. Ancient masonry towers are widely disseminated in Italy and represent one of the main elements of the local cultural heritage. In ancient times these structures were usually conceived mainly to resist vertical loads and are particularly vulnerable to earthquakes because of the limited ductility of masonry combined with the slenderness of the towers that are sometimes characterized by complex geometry and irregularities, [1–10]. The axial stresses due to gravity loads could be of the same order of magnitude as the compression strength of the old masonry and, when combined with the dynamic loads induced by earthquakes, can produce heavy damage and even local collapse. The prediction of the seismic response of historical masonry buildings represents a crucial issue and a challenging research item. An effective seismic vulnerability assessment of such structures can be obtained through non-linear dynamic and static analyses by means of suitable finite element (FE) models. In recent times, national [11–13] and international [14] codes have imposed the evaluation of the structural performance under horizontal loads, encouraging the use of sophisticated non-linear methods of analysis.

The paper, which can be considered as a thoughtful collection of case studies useful to infer general considerations, presents a comprehensive numerical study on the seismic performance assessment of eight historical masonry towers located in the North-East region of Italy. The towers exhibit different geometrical characteristics in terms of slenderness, cross-section area, openings, wall thickness and internal irregularities, but they are built with similar technologies and masonries presenting similar mechanical properties. Their structural behavior under horizontal loads may be therefore thought to be influenced mainly by geometrical issues.

Detailed three-dimensional finite element (FE) numerical models are created through the software package Abaqus [15] to represent the geometry of the towers. The main geometrical features of the towers are deduced from both existing available documentation and in-situ surveys. The evaluation of the seismic response of the historical masonry towers is carried out through non-linear dynamic analyses. A damage plasticity material model, exhibiting softening in both tension and compression, already

Article history:
Received 30 August 2015
Revised 19 January 2016
Accepted 3 February 2016

* Corresponding author. Tel.: +39 022399 4290; fax: +39 022399 4220.
E-mail address: milani@stru.polimi.it (G. Milani).

available in the commercial code Abaqus, is used for masonry. The seismic performance assessment of the towers is carried out in terms of displacement time history and tensile damage distribution. The effects of different geometrical characteristics and local irregularities on the seismic response of the towers are investigated.

A non-linear static procedure based on pushover analysis is also used for the seismic vulnerability assessment of the masonry towers. The results obtained by the two methods are compared in order to verify whether the simplified approach may represent the seismic behavior of the towers. A comparison between non-linear dynamic analyses and non-linear static procedures, even at a global level, can provide useful information about the seismic vulnerability of the towers. The effectiveness of the use of different approaches (non-linear static and dynamic analyses) for the seismic performance assessment of other typologies of structures is described in [16–21].

2. Description of the towers under study and FE models

This section provides a concise overview of the main geometrical and architectural features of the towers under study, along with some rough details on the FE discretization adopted. A general view, some geometric details and the FE models of the eight towers are presented from Figs. 1–8. The FE models of the eight towers (bell, clock or battle towers) are created directly in the commercial code Abaqus [15]. Three-dimensional elements are used to model masonry, with different material properties where necessary, to suitably take into account the presence of infill over the vaults or the possible central layer in multi-leaf walls. The choice of the element size is done in order to share the advantages of sufficiently reliable results and numerical efficiency during the non-linear dynamic analyses that usually needed very long time to be performed, even in workstations with large RAM. A preliminary size equal to 0.4–0.5 m is chosen for the sides of the 3D elements, with local or global refinements, depending on the specificity of the structure. Still, reasonable values of the mesh distortion are obtained, with a worst aspect ratio ranging between 2 and 3.

2.1. Clock tower of Trecenta (Tower I)

Tower I, see Fig. 1, is a civic tower located in Trecenta, a small town between Rovigo and Mantua, in Veneto region. The tower is entirely built in masonry, with regular bricks and regular texture. The height is about 22 m and the slenderness, defined as

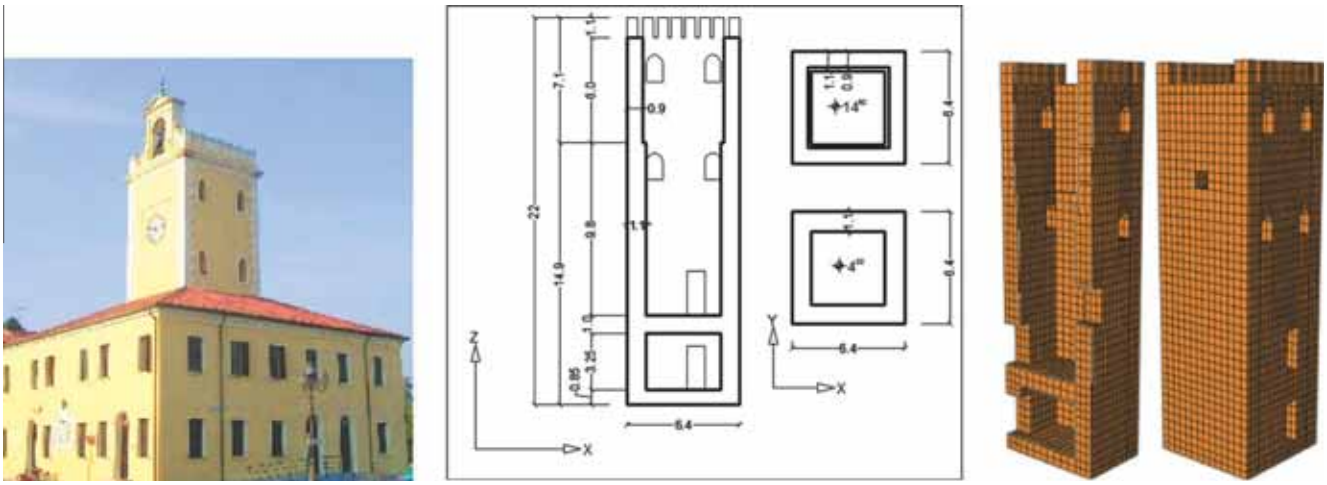

Fig. 1. Tower I: general view, geometric details and numerical FE model.

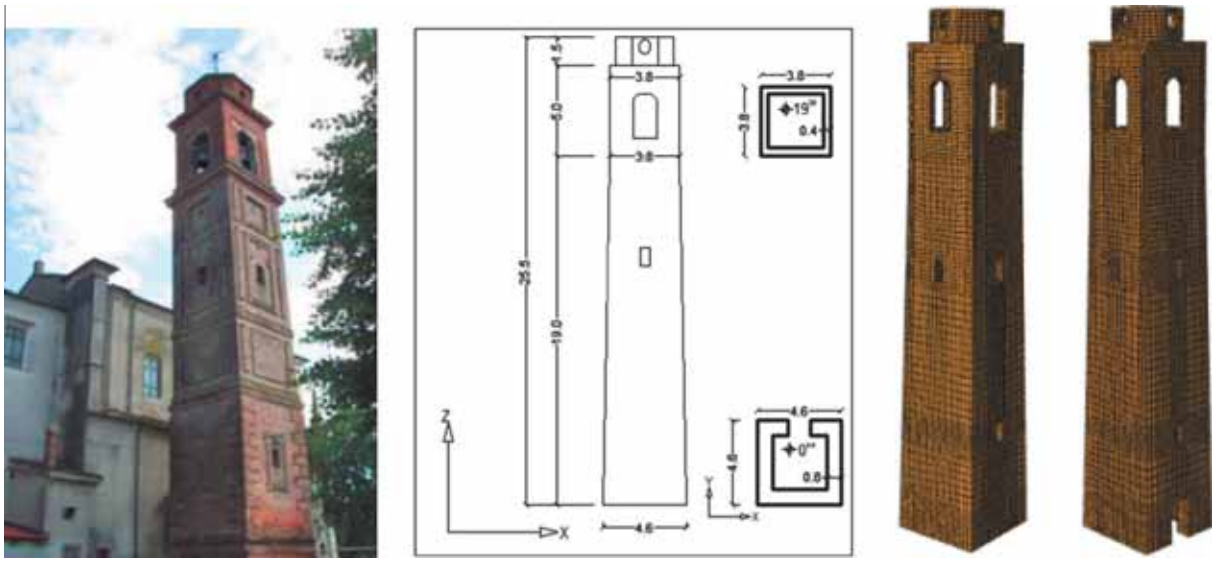

Fig. 2. Tower II: general view, geometric details and numerical FE model.

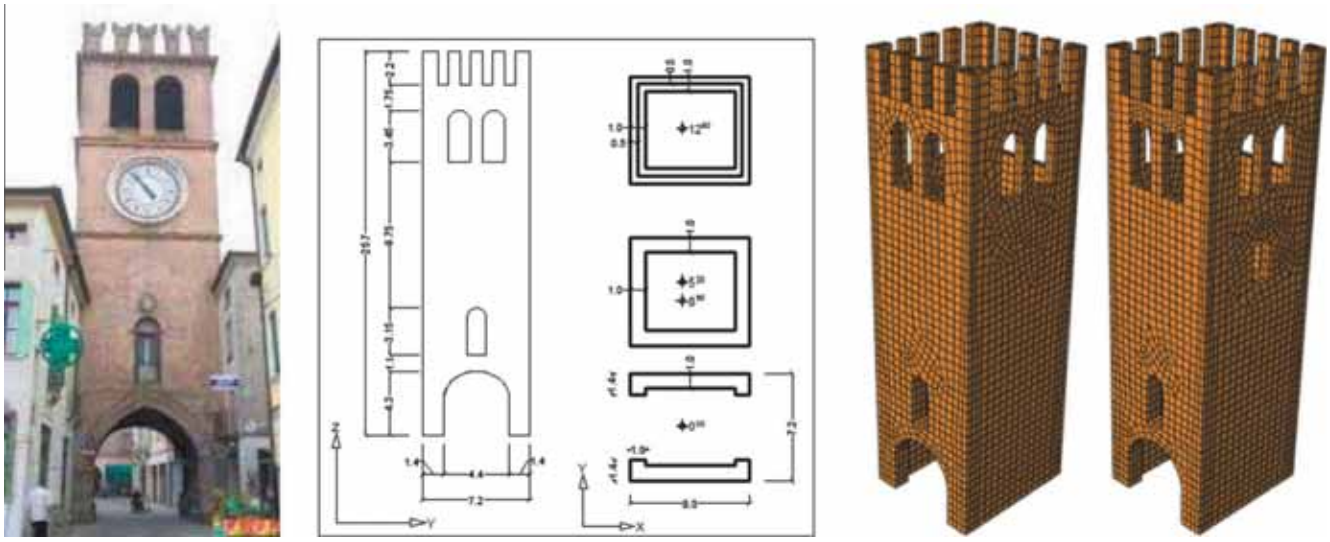

Fig. 3. Tower III: general view, geometric details and numerical FE model.

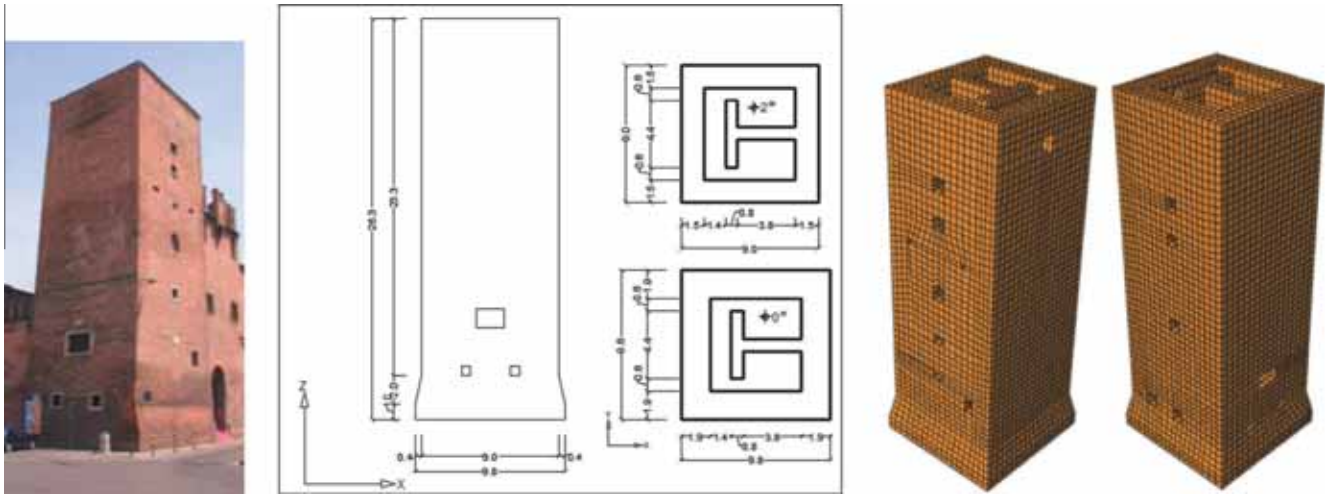

Fig. 4. Tower IV: general view, geometric details and numerical FE model.

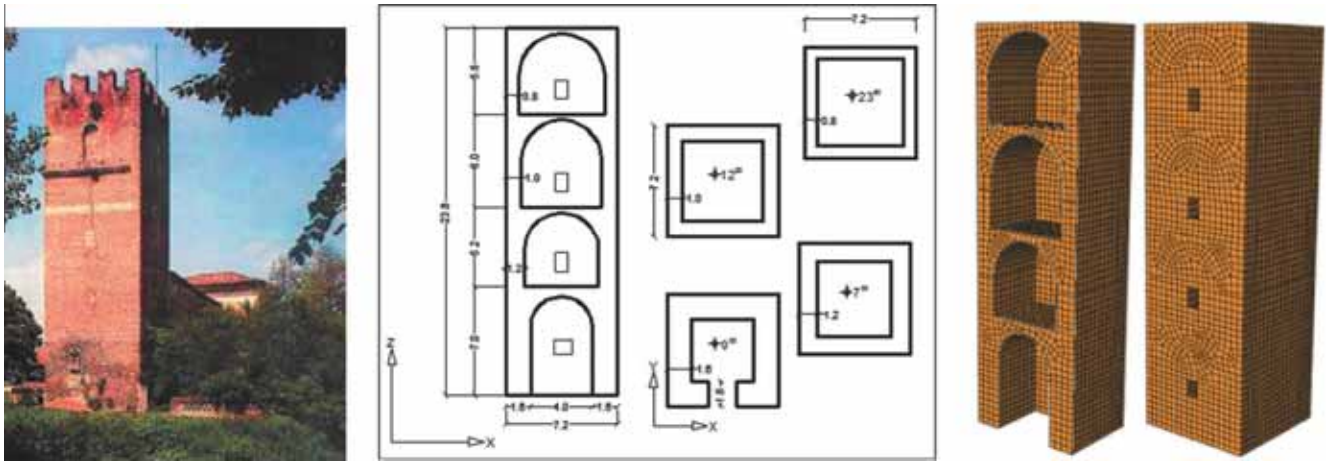

Fig. 5. Tower V: general view, geometric details and numerical FE model.

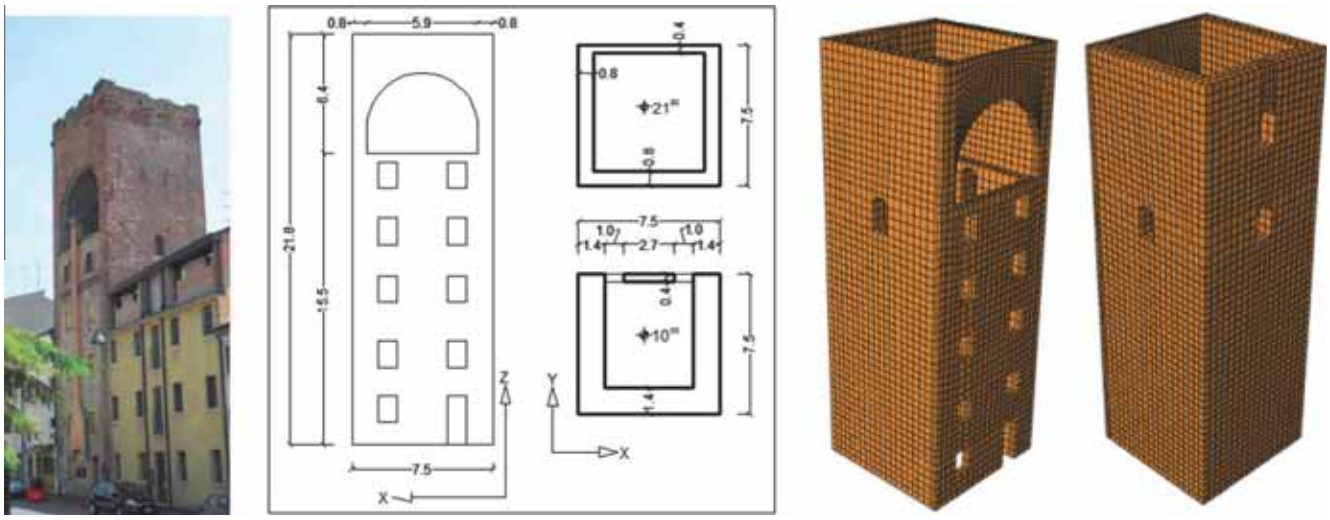

Fig. 6. Tower VI: general view, geometric details and numerical FE model.

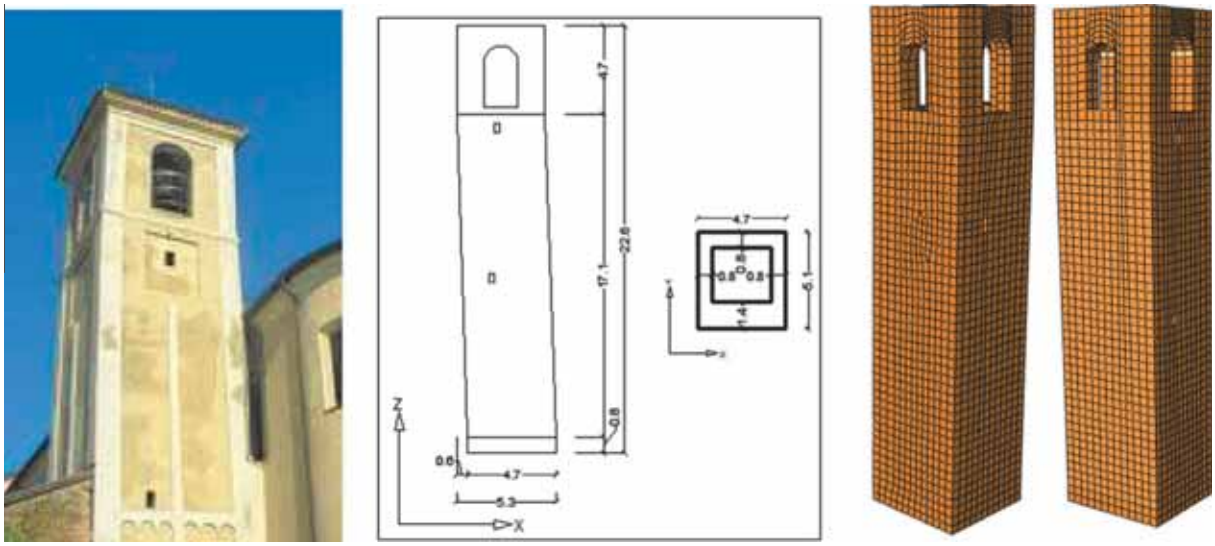

Fig. 7. Tower VII: general view, geometric details and numerical FE model.

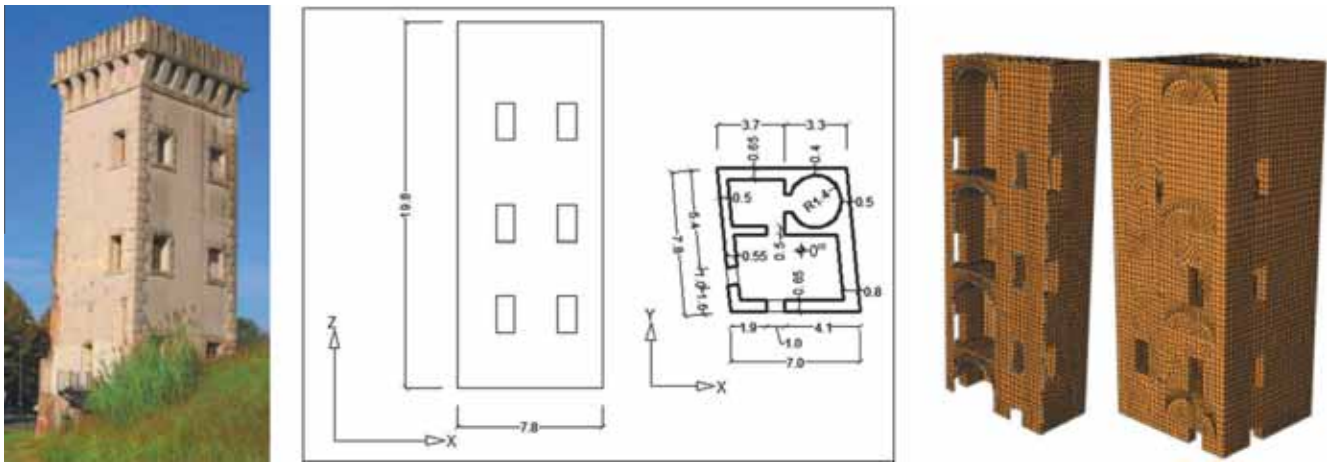

Fig. 8. Tower VIII: general view, geometric details and numerical FE model.

the ratio between the overall height of the structure and the smallest dimension of the base cross section, is roughly equal to 3.4. The tower is internally subdivided into six storeys, which are connected vertically by a wooden staircase. Each level is square in plan and consists of a unique space, which is partly occupied by the staircase. The ground floor is raised above the surrounding building through a slab with a thickness of 85 cm. For the first four floors the thickness of the perimeter walls is 110 cm, while for the last two is 90 cm. Most of the openings are located on the northern and southern façades.

2.2. Bell tower of San Giacomo church (Tower II)

Tower II, see Fig. 2, is a bell tower located in Polesine (Pegognaga), a small town in the province of Mantua in Lombardia region. Together with the church of San Giacomo Maggiore, it forms a complex of historical interest. During the recent Emilia-Romagna seismic event, it was severely damaged, with visible vertical cracks, a pattern that is typical for masonry towers subjected to horizontal loads. The bell tower, which dates back to the eighteenth century, has a square cross section with an external side of about 4.6 m. It presents an overall height of 25.5 m with a slenderness of about 5.5 and is internally subdivided into five floors. It was built entirely of regular small clay bricks with good mechanical properties. Walls, becoming gradually thinner from the bottom to the top, are 80 cm thick at the ground floor level and 40 cm thick at the top of the structure. Floors and stairs connecting the different levels are built in timber. Openings are present on all the façades. The structure is isolated, fully separated from the church that is situated a few meters away. This feature excludes the possibility of any interaction between the two structures during the analysis under horizontal loads. As a consequence, the damage caused by the recent Emilia-Romagna earthquake depends exclusively on the characteristics of the tower itself and on the seismic event. The damage observed after the seismic sequence is mainly concentrated along vertical lines of weakness, located in correspondence with the openings that indeed are vertically aligned. The most relevant damage is registered on the north-East and the south-west parallel façades. After visual inspection, the texture appears extremely regular, with a good interconnection between perpendicular walls.

2.3. Clock tower in Lendinara (Tower III)

Tower III, see Fig. 3, is a military city tower located in Lendinara, a town near Rovigo in Veneto region. The tower, which in ancient times represented the gate of the town, is nowadays the connection between two small squares. It has a height equal to about 26 m and the slenderness is about 3.6. It exhibits an almost square plan and is internally subdivided into five storeys, plus one detectable mezzanine between the third and the fourth level. The tower is built entirely by bricks with a regular shape assembled in a very regular texture. The thickness of the walls is equal to 100 cm for the first two floors and to 50 cm for the upper part of the structure. The eastern and western façades are almost identical, both decorated with a clock and adorned with wooden frames and terracotta. It presents some internal irregularities for the presence of two arches at the ground floor, as depicted in Fig. 3. On the top there is a large double opening on each side of the structure. The tower is decorated by merlon elements, highlighted by a stylish notched frame. The structure needs some restoration interventions, especially to strengthen the floors and the roof.

2.4. Maistra tower of Praetorian Palace (Tower IV)

Tower IV, see Fig. 4, is located in Lendinara, as the previous one. The original tower was built in crenelated style, with clay bricks regular in shape. The tower has a height of about 26.3 m and is one of the highest towers in the region of Polesine. The slenderness is about 2.9. In elevation the building is divided into five storeys and there is a detectable mezzanine between the ground and the first floor, connected by a wooden staircase. The tower is almost square in plan and there is an internal subdivision into three rooms – two small ones and a hallway. All the ceilings are made of wood boards, but only the first floor has its original terracotta tiles. The thickness of the walls is 150–190 cm and is constant along the height of the tower. The structure stands on a tapering upwards base. The openings of the ground, mezzanine and first floors are small and have square shape. In the past the tower was crowned by merlon elements (found in several ancient maps).

2.5. Tower of Treves castle (Tower V)

Tower V, see Fig. 5, is located in Arquà Polesine, a small town between the cities of Rovigo and Ferrara in Veneto region. The tower, which dates back to the twelfth century and belongs to Este castle (now Treves castle), received some important amendments during the centuries but globally preserves its original medieval character. The height of the structure is equal to 24 m and the slenderness is about 3.3. Vertically, the internal space is subdivided into four storeys, connected by a narrow stone-made stair. Each storey has a square plan, consisting of a single compartment and a barrel-vaulted ceiling. The thickness of the walls changes in correspondence with each level as follows: 160 cm, 120 cm, 100 cm and 80 cm on the ground, first, second and third floor, respectively. Some of the arches and the windows of the original design are now buffered and others have been modified. On the third floor of the western and eastern prospects, there is an arch that was buffered long time ago. The northern prospect, from the ground floor to the third, is characterized by the presence of a window with a round arch at its top, which was modified later and now the windows have a square shape. There are stringcourse marks below the ceiling of the third floor. All the prospects are decorated with merlon elements on the top of the tower. Due to its historical and architectural importance, an urgent restoration of both internal and external parts is needed, which would bring back its original configuration.

2.6. Pighin tower (Tower VI)

Tower VI, see Fig. 6, is a defence tower located in Rovigo in Veneto region. Since the tower was built (twelfth century) as a Medieval defence structure, it was totally opened toward the city. With the evolution of the military technology, the tower lost its strategic importance and around 1775 the missing wall was filled when the structure became a part of a residential building. Pighin tower, whose real name is “St. Augustine door”, presents a height equal to 21.8 m and the slenderness is about 2.9. It is internally subdivided into six floors. Originally, it had wooden slabs, connected by ladders. Each of the floors has a square plan and consists of a single compartment. Three walls have a thickness of 140 cm for the first five storeys and a thickness of 80 cm for the last storey, whereas the thickness of the wall that was built later is equal to 40 cm for the whole height of the structure. The eastern and western facades are almost identical; there is also a quite unusual chimney on the northern façade, added when the tower became a residential building. The structure that can be seen today is almost the original one, dating back to the eighteenth century. A recent restoration was done in 1983, mainly consisting of light re-stitching of the mortar joints.

2.7. Bell tower of San Sisto II church (Tower VII)

Tower VII, see Fig. 7, is a bell tower belonging to the church of San Sisto II in Palidano, a small town between the cities of

Modena and Mantua in Lombardia region. The structure is built in Romanesque style and exhibits a height of 22.6 m and the slenderness is about 4.8. It is internally subdivided into six storeys, with wooden floors connected by a wooden staircase. All of the floors are approximately square in plan (4.7/5.1 m) and consist of a unique space, which is partly occupied by the staircase. The tower exhibits a marked inclination with a horizontal displacement of the top section centroid equal to about 0.6 m at a height of 17 m. The thickness of the four perimeter walls is constant along the height and equal to 1.4 m for one of the walls and 0.8 m for the others. The bell is framed by a belfry with large arched windows. The other openings are very small and located in the western and eastern façades only.

2.8. Morosini tower (Tower VIII)

Tower VIII, see Fig. 8, is located in Lusia, a small town in the province of Rovigo in Veneto region. In the past, the tower belonged to a magnificent complex known as Morosini Villa. Now, it is the only evidence of such a complex, that was completely destroyed during the second world war. The tower presents a height of about 20 m and the slenderness is about 2.8. It is internally subdivided into four storeys (one of them is a basement), connected by a spiral wooden staircase. Every floor consists of three rooms - one of them occupied by the staircase and the other two having magnificent vault ceilings. The walls have a thickness of 40–80 cm. Externally, the corners between the walls, the windows and the doors are adorned by a decorative ashlar. The stone blocks are apparently of good quality and well-preserved. The traces of the junction of the tower with the surrounding buildings can be still seen (with the main building through the western wall and with a small building through the southern wall) – in particular, the punctures due to the intersection of the beams and the strips. The tower is crowned by battlements. In 1998 a restoration intervention was performed, still not finished for budget limitations. At present, new signs of deterioration can be seen, so far limited, but showing that there is the need to take some appropriate rehabilitation measures.

3. The material model adopted

Masonry arranged in a regular texture is well recognized to behave in a rather complex way, exhibiting orthotropy along material axes, marked damage in tension with very low strength, different failure surfaces in tension and compression, plastic deformation with damage during crushing in compression, softening and so on. Some of the main features of such a complex material have been recently well approximated by different numerical models under static loads, for instance in [22–24], but the implementation of efficient and ready models for commercial codes is still under development. One of the main obstacles is represented by the fact that masonry is too much peculiar with regard to texture (regular or irregular, and if regular, in dependence of the actual disposition of the bricks used), typology of units (concrete, clay, perforated or not, shape), regularity of units, eventual presence of infill in multi leaf walls, etc.

Basing on such premises, it appears clear that the utilization of sophisticated models from specialized literature, which proved to be very effective in specific cases, is not possible in common design practice. As a consequence, it is usually accepted to adapt damage-plasticity isotropic models conceived mainly for concrete to the masonry case. In this way, the orthotropic behavior is completely lost, but average strength and stiffness values along the material axes are used, so that the overall behavior of the structure is marginally affected by such inaccuracy. On the other hand, both damage in tension and crushing in compression may be easily handled with a material model framework that proved good stability in a variety of different problems, including analyses under seismic excitation, an issue that appears crucial when masonry structures in earthquake-prone areas are considered.

It is worth noting that Italian Guidelines on Cultural Heritage [13] explicitly state that the utilization of 3D FE models is recommended, considering suitable constitutive models for masonry. Such models should be capable of reproducing the typical strength and stiffness degradation exhibited by the masonry material in the inelastic range.

Basing on such information and code of practice requirements, in what follows the 3D FE models of the towers are implemented into Abaqus [15] taking into consideration geometrical (large displacement effects) and material non-linearity by means of the Concrete Damage Plasticity (CDP) model, fully available in the standard package.

Concrete Damage Plasticity model is based on the assumption of a scalar isotropic damage with distinct damage parameters in tension and in compression. It is particularly suitable for applications in which the material exhibits damage, especially under loading–unloading conditions, and therefore for seismic analyses. A different inelastic behavior in tension and compression is then introduced, as shown in Fig. 9.

To describe the multi-dimensional behavior in the inelastic range, masonry is assumed to obey a Drucker–Prager strength criterion with non-associated flow rule. The strength domain is a standard Drucker–Prager surface modified by means of the so-called K_c parameter, representing the ratio between the second stress invariant on the tensile meridian and that on the compressive meridian, Fig. 10. This parameter is set equal to 0.666 in the numerical simulations.

A value equal to 10° is adopted for the dilatation angle, which seems reasonable for masonry subjected to a moderate-to-low level of vertical compression. This value is in agreement with experimental evidences available in the literature. To avoid numerical convergence issues, the tip of the conical Drucker–Prager strength domain is smoothed using a hyperbola. Abaqus code allows for smoothing the strength domain by means of the so-called eccentricity parameter, which represents the distance between the points of intersection with the p-axis of the cone and the hyperbola in the p–q plane, where p is the hydrostatic pressure stress and q is the Mises equivalent stress, see Fig. 11. A value equal to 0.1 is adopted for the eccentricity parameter in the numerical simulations.

The available experimental results on regular masonry wallets show a moderate orthotropy ratio (around 1.2) under biaxial stress states in the compression–compression region [25]. Obviously, such feature cannot be taken into account when an isotropic model, like the present one, is utilized. However, it is commonly accepted in the literature the utilization of isotropic models (like concrete smeared crack approach available in both Ansys and Adina software codes) after an adaptation of the parameters to fit an average behavior between vertical and horizontal compression. A suitable model should also take into account the ratio between the ultimate compression strength in biaxial stress states and in uniaxial conditions. Such a ratio, which exhibits similar values for concrete and masonry, is reasonably set equal to 1.16. The values of the various parameters adopted for the numerical simulations are reported in Table 1.

The final stress–strain relationship in tension adopted for the dynamic analyses follows a linear-elastic branch up to the peak stress σ_{t0}. Then, micro-cracks start to propagate within the material, leading to a macroscopic softening. In compression, the response is linear up to the yield stress σ_{c0}. Then, a linear hardening is assumed up to the crushing stress σ_{cu}, followed by a linear softening branch.

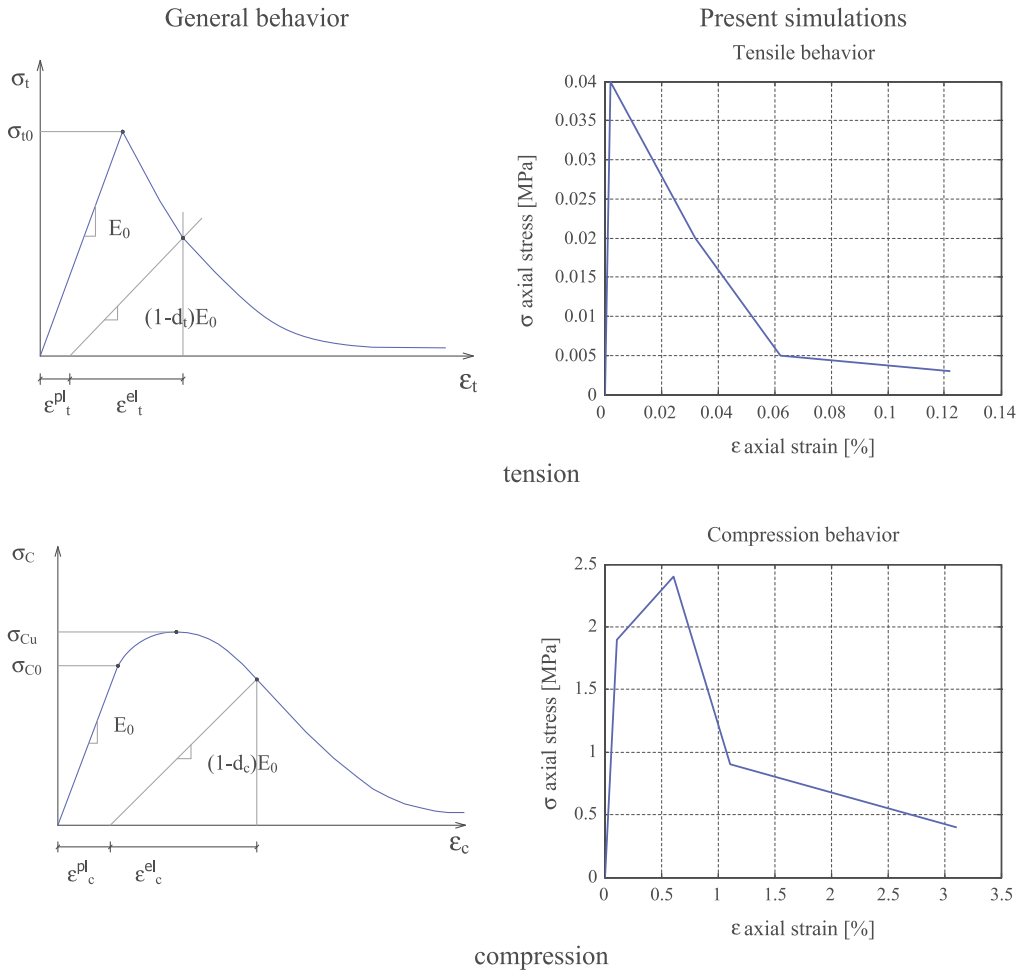

Fig. 9. Constitutive law in tension and compression adopted for masonry.

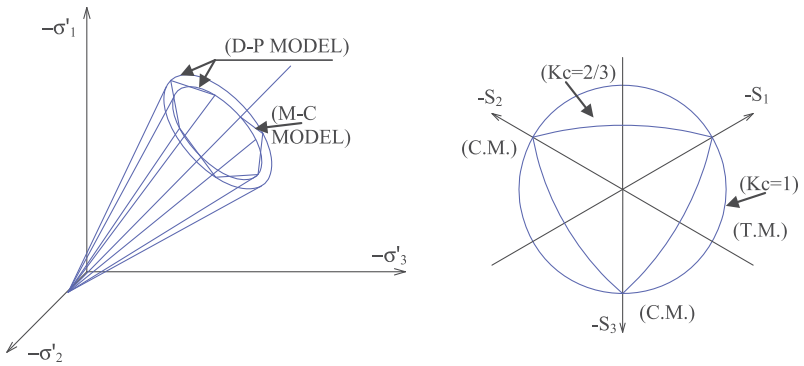

Fig. 10. Modified Drucker–Prager strength domain.

The damage variables in tension d_t and compression d_c are defined by means of the following standard relationships:

$$\sigma_t = (1 - d_t)E_0(\varepsilon_t - \varepsilon_t^{pl})$$
$$\sigma_c = (1 - d_c)E_0(\varepsilon_c - \varepsilon_c^{pl}) \quad (1)$$

where $\sigma_t(\sigma_c)$ is the uniaxial tensile (compressive) stress, E_0 is the initial elastic modulus, $\varepsilon_t(\varepsilon_c)$ is the uniaxial total strain in tension (compression), $\varepsilon_t^{pl}(\varepsilon_c^{pl})$ is the equivalent plastic strain in tension (compression). In the present study, only tension damage is assumed to be active, because the adopted tensile strength of the material is significantly lower than the compressive strength. When the strain reaches a critical value, the material starts to degrade showing, in the unloading phase, a modulus equal to $E < E_0$. In particular, in the numerical simulations conducted in this study a reduction equal to 5% of the Young modulus with respect to the initial value is assumed for a plastic deformation equal to 0.003.

The issue of mechanical properties to adopt for the constituent materials is very tricky. It is common opinion, indeed, that the major damages registered in historical buildings, such as towers, castles and churches, are a consequence of very poor mechanical properties of joints, whereas clay bricks exhibit a quite high strength in such Italian region.

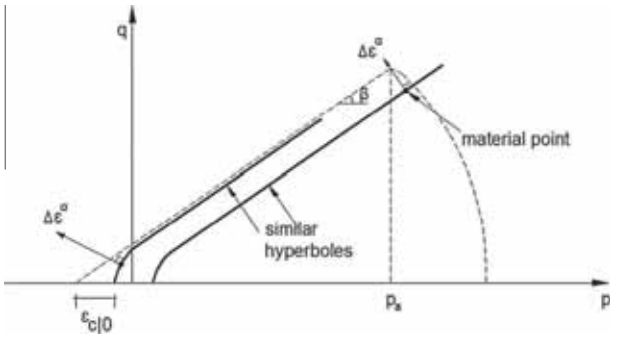

Fig. 11. Smoothed Drucker–Prager failure criterion adopted in the numerical simulations, p–q plane.

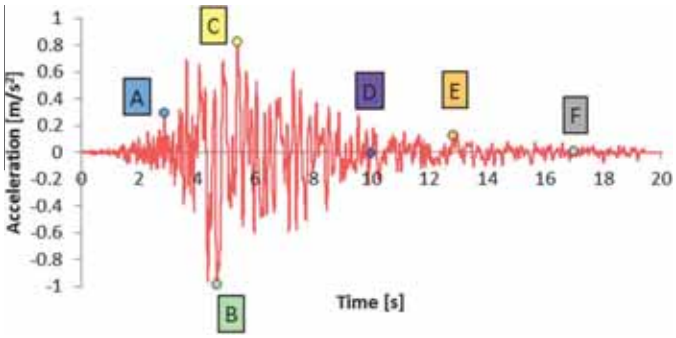

Fig. 12. Scaled real accelerogram used in the non-linear dynamic analyses and meaningful points used to evaluate the state of damage of the towers under study.

Table 1
Values of the mechanical parameters adopted for the numerical simulations.

Parameter	Value
Poisson's ratio	0.2
Dilatation angle	10°
Eccentricity	0.1
σ_{b0}/σ_{c0}	1.16
K	0.666
Viscosity parameter	0.002

In the absence of ad-hoc experimental campaigns performed on the case studies at hand, it is necessary to refer to what is stated by Italian Code for existing masonry buildings.

As a matter of fact, masonry is a material which exhibits distinct directional properties due to the mortar joints, acting as planes of weakness.

Considering the well-known limitation of the use of both micro-modelling and homogenization at large scale, isotropic macro-models are adopted for masonry. The reason for adopting an isotropic material stands in the impossibility to evaluate many parameters necessary for anisotropic materials in the inelastic range, in the absence of ad-hoc experimental characterizations. Finally, it is worth noting that commercial codes rarely put at disposal to users anisotropic mechanical models suitable to describe masonry with a regular texture in the non-linear range.

According to Italian Code NTC 2008 [11] and subsequent Explicative Notes [12], the mechanical properties assumed for masonry material depend on the so-called knowledge level LC, which is related to the so-called Confidence Factor FC. There are three LCs, labeled from 1 to 3, related to the knowledge level about the mechanical and geometrical properties of the structure. The knowledge level LC3 is the maximum, whereas LC1 is the minimum. For the cases at hand, a LC1 level is assumed in the absence of specific in-situ test results.

As a consequence, the values adopted for cohesion and masonry elastic modulus are taken in agreement with Explicative Notes [12] for the application of the Italian Code NTC 2008 [11], assuming a masonry typology constituted by clay bricks with very poor mechanical properties of the joint and quite regular courses. The stress–strain relationships adopted in the ABAQUS model are therefore those depicted in Fig. 9, which (where data are available) are in agreement with the Italian code requirements.

4. Analyses performed

Two different numerical approaches, namely non-linear static procedure based on pushover analyses and non-linear dynamic analysis, are carried out in this study, with a level of numerical complexity that can be considered ranging from moderately high to high in common design practice. In a companion paper [26], considerations on the seismic vulnerability of the towers by means of eigen-frequency analyses associated with response spectrum, evaluation of the seismic safety Index by means of the simplified sectional approach suggested in the Italian Guidelines for built heritage [13] and non-linear static procedures are discussed in detail. In this study only the results of the non-linear dynamic analyses are presented and compared with the non-linear static procedure for the sake of conciseness.

4.1. Non-linear dynamic analyses

Non-linear dynamic analyses are performed as follows: in the first step, gravity loads are slowly applied to the structure without any ground acceleration; in the second phase, the horizontal ground motion is applied at the base of the structure along with pre-existing gravity loads. It has been indeed shown in many technical papers, see e.g. [1–10], that the application of the vertical component of the ground motion is important mainly for tall towers, i.e. where the height exceeds 40–50 m, which is not the present case. The real accelerogram registered in Mirandola on the 20th of May 2012 during the Emilia-Romagna seismic event is used to investigate the seismic response of the towers under study. The accelerogram is appropriately scaled in order to obtain two acceleration time histories with different values (0.1 g and 0.2 g) of the peak ground acceleration (PGA). Fig. 12 shows the acceleration time history with PGA = 0.1 g along with some meaningful instants identified with different letters and colors. The chosen instants are the following: instant A (blue[1]) is the first relevant ground motion acceleration peak, instant B (green) is the negative acceleration peak, instant C (yellow) is the positive acceleration peak, instant D (purple) is the half time of the recorded ground motion, instant E (orange) is the last relevant ground motion acceleration peak and instant F (gray) represents the practical end of the seismic excitation.

It can be noted that not all the dynamic simulations are carried out up to instant F. As a matter of fact, some of them, especially for PGA = 0.2 g, are aborted at control node displacements incompatible with the capacity of the tower, a clear indication of the incipient collapse of the structure. In such cases, the damage contour plot reported in what follows does not correspond obviously to instant F, but to the time where numerical simulations are interrupted. The choice to analyse the behavior of the towers for PGA = 0.2 g was made because authors experienced in several cases a sufficient ability to withstand the seismic excitation (both using non-linear static procedure and non-linear dynamic analyses) for PGA = 0.1 g. The dynamic analyses are performed applying the accelerogram, separately, along the two principal (X and Y)

[1] For interpretation of color in Fig. 12, the reader is referred to the web version of this article.

directions of each tower. The horizontal displacement time histories of some control points, normally the nodes at the top of the towers, along with the damage state at the end of the simulations, are used to qualitatively determine if the structure is in a state of incipient collapse or not. The numerical analyses are carried out by means of a dynamic approach with implicit integration in the time domain, using a time step equal to 0.005 s, which corresponds to the accelerogram registration time interval. The main results of the non-linear dynamic analyses conducted in this study are reported in the following sections.

4.2. Non-linear static procedure

A simplified assessment procedure is also adopted for the seismic verification of the global structural behavior of the towers under study. The procedure was developed at the University of Ljubljana by Fajfar [27] and is based on pushover analyses and on inelastic demand spectrum. This simplified method of analysis is an effective technique for the seismic assessment of existing structures and combines pushover analysis of a multi-degree-of-freedom (MDOF) model with the response spectrum analysis of an equivalent single-degree-of-freedom (SDOF) model. The method is formulated in the acceleration–displacement (AD) format, which enables the visual interpretation of the results. By means of a graphical procedure, the capacity of a structure is compared with the demand of an earthquake ground motion on the same structure, Fig. 13.

The capacity of the structure is represented by a force–displacement curve obtained by non-linear static analysis. According to Italian Code [11,12], when dealing with pushover analyses, the response of the structure should be investigated along the geometrical orthogonal axes X and Y, in both the positive and negative directions. Italian Code also prescribes the evaluation of the load carrying capacity by means of two configurations of horizontal forces: the first, denoted as G1, provides a distribution of forces derived by the assumption of a linear variation of acceleration along the height, while the second, denoted as G2, assumes a uniform acceleration pattern. For the towers under consideration, according to authors' experience, distribution G1 provides collapse accelerations lower than those provided by distribution G2, therefore the reduction of the system to a SDOF system is always done with reference to distribution G1. In the cases of different structural behavior along the positive and negative directions (e.g. $+X$ and $-X$, or $+Y$ and $-Y$), the more conservative results are presented. Distributions G1 and G2 are automatically applied to ABAQUS meshes by means of user defined "body forces" functions. The base shear is plotted against the displacement of a control point belonging to the roof, having experienced a quite global flexural/shear collapse mode during non-linear static analyses. The capacity curve of the structure is transformed into the capacity curve of an equivalent SDOF system by means of the transformation factor $\Gamma = \sum m_i\phi_i / \sum m_i\phi_i^2$, where ϕ_i is the ith component of the eigenvector $\mathbf{\Phi}$ deduced from modal analysis and m_i is the mass of the node i. The capacity curve of the equivalent SDOF system is then reduced to a bilinear elastic-perfectly plastic force–displacement diagram on the basis of the equal energy concept (the areas underneath the actual and bilinear curves are approximately the same, within the range of interest). The elastic stiffness of the idealized bilinear curve is computed by drawing a line from the origin to the point of the equivalent capacity curve at a base shear equal to 70% of the peak base shear. The equivalent capacity curve is stopped at a displacement corresponding to a base shear equal to 85% of the peak base shear. As usually occurs in complex 3D non-linear analyses, a softening of about 15% is hardly reproducible. Italian Guidelines on Cultural Heritage [13], considering

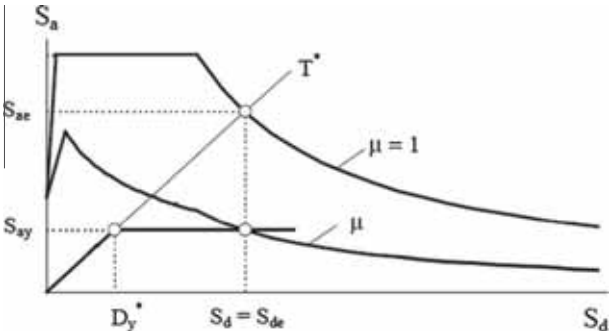

Fig. 13. Elastic and inelastic demand spectra versus capacity diagram in acceleration–displacement (AD) format. Notation: S_{ae} and S_{ay} are, respectively, the accelerations corresponding to the elastic and inelastic systems; D_y^* is the yield displacement; S_d and S_{de} are, respectively, the inelastic and elastic displacement demand; T^* is the period of the idealized bilinear system; μ is the ductility demand.

the difficulties in the definition of the displacement at the ultimate limit state, recommend carrying out analyses up to meaningful displacements, which may be reasonably associated with the activation of a failure mechanism. It is also recommended to evaluate the ratio between the elastic limit base shear and the ultimate base shear of the bilinear system. Such a ratio shouldn't exceed a maximum admissible value defined on the basis of the ductility and dynamic features of each structural typology.

The elastic acceleration S_{ae} and the corresponding elastic displacement demand S_{de} are computed by intersecting the radial line corresponding to the elastic period of the idealized bilinear system with the elastic demand spectrum. In all the cases analyzed in this study the elastic period of the bilinear system is larger than T_C (the upper limit of the period of the constant spectral acceleration branch) and the inelastic displacement demand S_d is equal to the elastic displacement demand S_{de}.

The displacement capacity corresponds to the end point of the bilinear curve. The inelastic demand in terms of accelerations and displacements is provided by the intersection point of the capacity curve with the demand spectrum corresponding to the ductility demand μ, as schematically shown in Fig. 13. In this study, the seismic demand is computed with reference to the Eurocode 8 response spectrum (soil type C). The theoretical predictions are performed for Sa_g levels equal to 0.1 g and 0.2 g. The displacement demands refer to the equivalent SDOF system. The displacement demands of the structure are obtained by multiplying the displacement demands of the SDOF system by the transformation factor Γ. Seismic assessment is performed by comparing displacement capacity and demand. The main results of the non-linear static procedure are reported in Section 6 for a direct comparison with the results of the non-linear dynamic analyses.

5. Numerical results of non-linear dynamic analyses

The displacement time histories of the control nodes obtained in all the different cases (X and Y directions, accelerograms with PGA equal to 0.1 g and 0.2 g) by means of the non-linear dynamic analyses are presented from Figs. 14–21.

In particular, the response of the towers under an accelerogram with PGA equal to 0.1 g is presented from Figs. 14–17. Figs. 14 and 15 refer to the X direction, Figs. 16 and 17 refer to the Y direction.

Analogously, the displacement time histories obtained with the application of the accelerogram with PGA equal to 0.2 g are depicted from Figs. 18–21. Analogously to the previous case, Figs. 18 and 19 refer to the X direction, Figs. 20 and 21 to the Y direction.

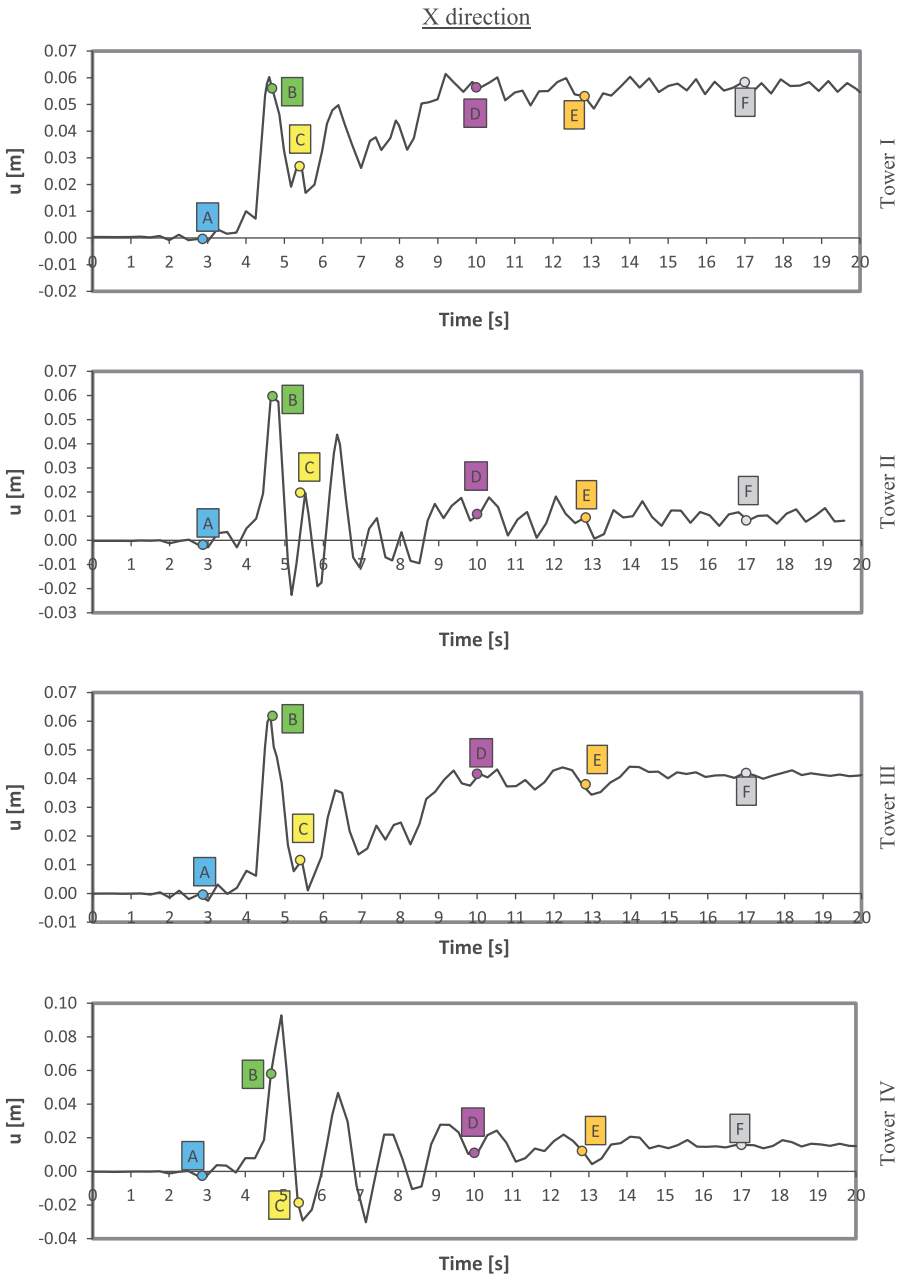

Fig. 14. Non-linear dynamic analyses, *X* direction, PGA = 0.1 g. Displacement time history diagram for Towers I–IV.

It can be roughly stated that if a residual deformation, defined as the ratio between the horizontal inelastic residual displacement and the height of the tower, ranging between 0.4% and 0.8% is reached, the structure may be reasonably considered in incipient state of collapse. Values of 0.4% and 0.8% of residual deformation are taken with reference to masonry piers behavior at failure under in-plane bending and shear, respectively, in agreement with Italian code specifics. While such a choice is rather debatable, because masonry towers can be hardly thought to behave as single piers, it is probably the only quantitative indication that can be attempted in this case.

The inelastic residual deformations obtained for all the cases investigated are synoptically shown in Fig. 22, where threshold values of 0.4% and 0.8% are also indicated. The maximum values of the top displacements normalized to the height of the towers are summarized in Fig. 23. In the same figures, front view sketches and indications of the heights of the towers under study are reported for the sake of clarity.

The displacement time histories for Tower I show that the peak values of the top displacement are larger in the *X* direction than in the *Y* direction and inelastic residual deformations are critical in the *X* direction under seismic excitation with PGA = 0.2 g.

The maximum values of the top displacements of Tower II are non-negligible and similar in both the directions under seismic excitations with PGA = 0.1 g and PGA = 0.2 g. Top displacement time histories under PGA = 0.2 g show negligible inelastic residual deformations in both the *X* and *Y* directions.

The top displacement time histories for Tower III subjected to seismic excitation with PGA = 0.2 g tend to diverge in the *Y* direction and relevant inelastic residual deformations are observed in

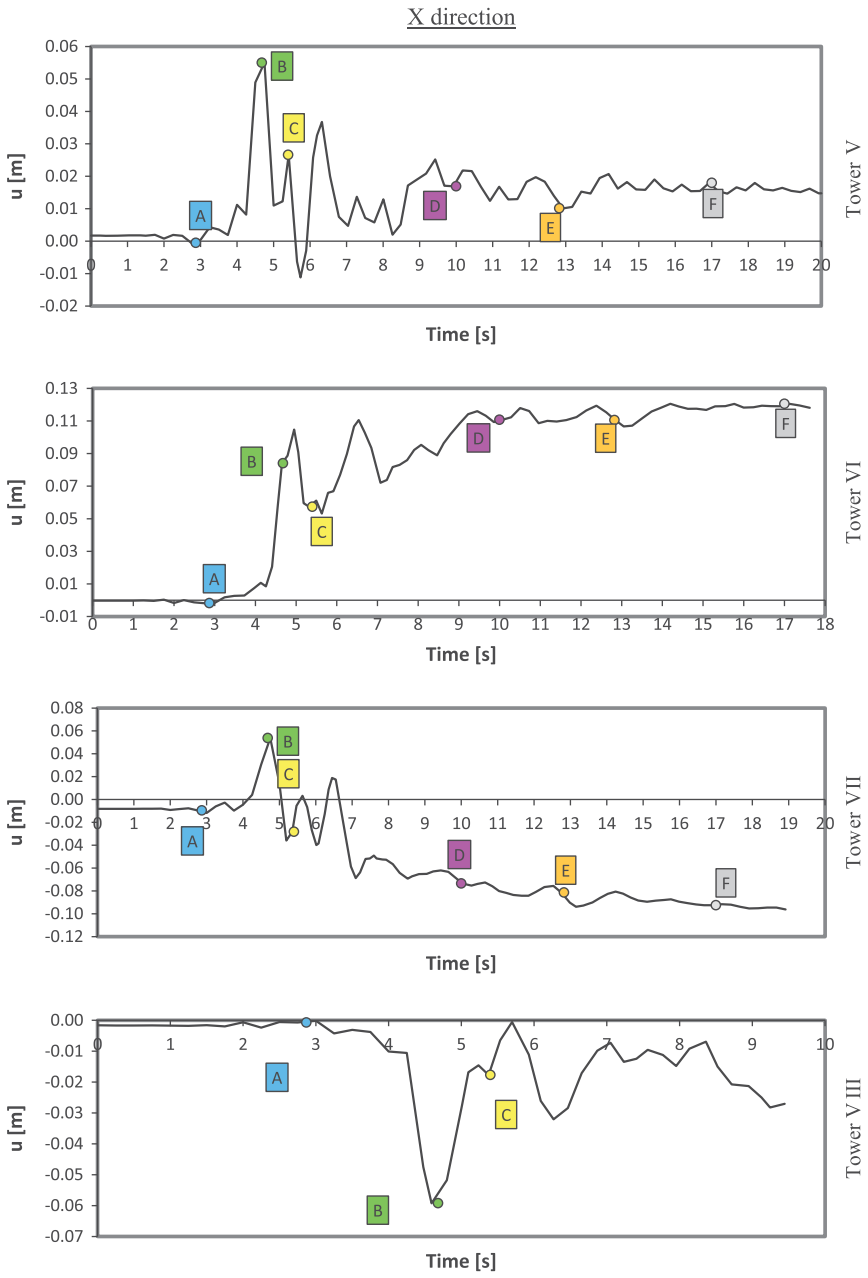

Fig. 15. Non-linear dynamic analyses, *X* direction, PGA = 0.1 g. Displacement time history diagram for Towers V–VIII.

both the *X* and *Y* directions. There is a marked difference between the horizontal top displacements in the two orthogonal directions.

Tower IV exhibits non-negligible maximum values of the top displacements under seismic excitation with PGA = 0.2 g. Top displacement time histories show limited inelastic residual deformations.

Very large top horizontal displacements are registered for Tower V even in the case of dynamic simulation with PGA = 0.1 g in the *Y* direction. Top displacement time histories under PGA = 0.2 g tend to diverge and present relevant inelastic residual deformations in both the *X* and *Y* directions.

Tower VI shows large top displacements, along with important inelastic residual deformations, in the *X* direction even in the case of dynamic simulation with PGA = 0.1 g.

Large maximum horizontal displacements in the *X* direction are registered for Tower VII subjected to seismic excitation with PGA = 0.1 g. Top displacement time histories under PGA = 0.2 g tend to diverge in the *X* direction and show relevant inelastic residual deformations. There is a marked difference between the horizontal top displacements in the two orthogonal directions. On the basis of the dynamic simulations carried out, it can be noted that the inclination makes the structure vulnerable to damage even under PGA = 0.1 g.

The maximum values of the top displacements are critical in the *Y* direction for Tower VIII under seismic excitation with PGA = 0.2 g. Top displacement time histories under PGA = 0.2 g show relevant inelastic residual deformations in the *Y* direction.

From an overall analysis of the results of the dynamic simulations with two different PGAs, the following remarks may be drawn.

Under seismic excitation with PGA = 0.1 g, it can be noted that Tower I, Tower II, Tower III, Tower IV and Tower VIII exhibit values

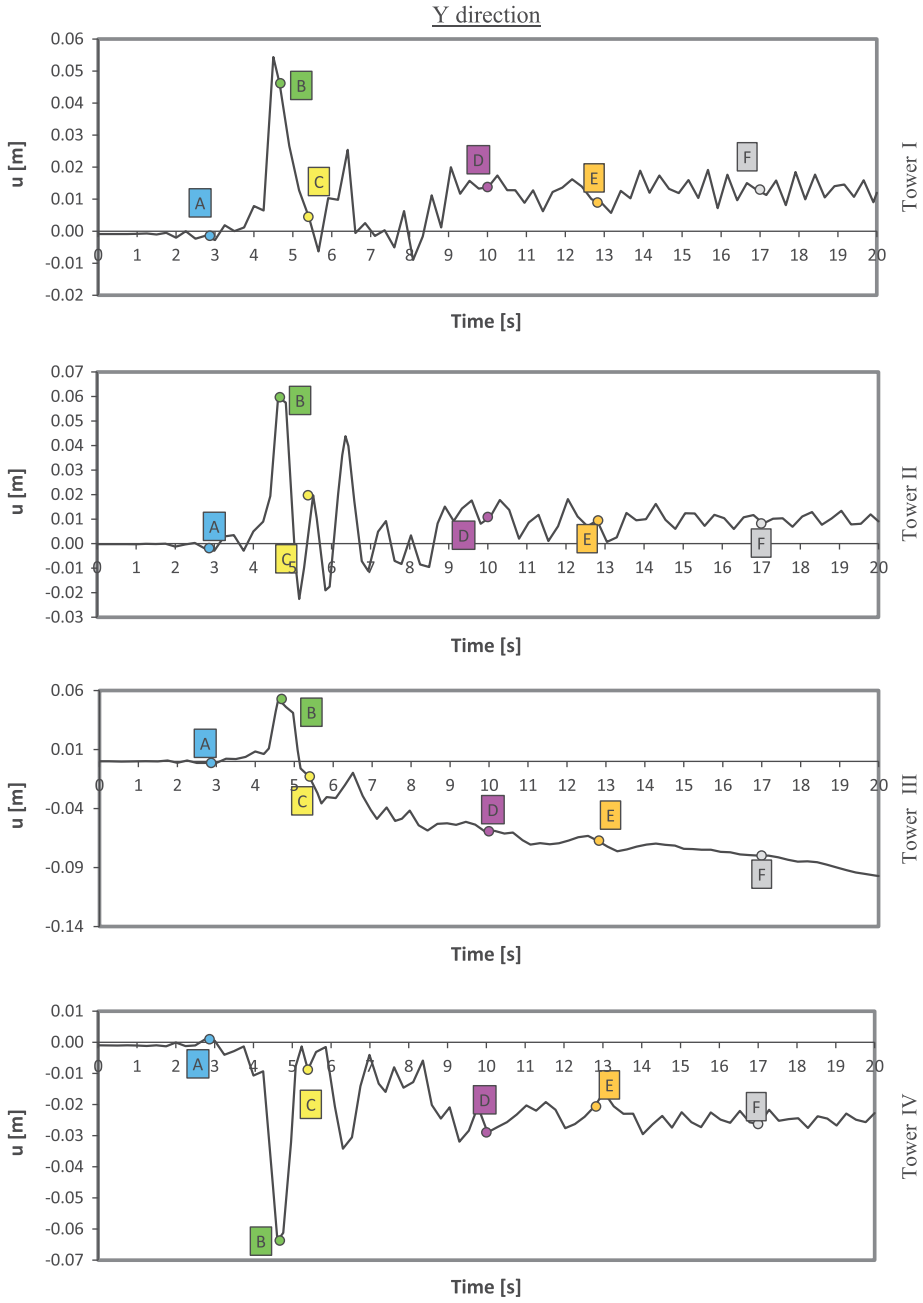

Fig. 16. Non-linear dynamic analyses, *Y* direction, PGA = 0.1 g. Displacement time history diagram for Towers I–IV.

of residual deformations smaller than 0.4% of the height. It can be observed that the values of residual deformation are critical (within 0.4–0.8%) for Tower VI and Tower VII; Tower V can be considered as prone to collapse. These results are confirmed in terms of non-dimensional top displacements.

Under seismic excitation with PGA = 0.2 g, basing on the criterion of inelastic residual deformations, a collapse mechanism is activated for Tower III, Tower V, Tower VI, Tower VII and Tower VIII. The values of residual deformations are critical (within 0.4–0.8%) for Tower I; Tower II and Tower IV exhibit acceptable residual deformations (smaller than 0.4% of the height). These results are confirmed in terms of normalized top displacement, but also Tower II and Tower IV present non-dimensional top displacement within 0.4–0.8%.

6. Comparison with results obtained by the non-linear static procedure

The results of the non-linear static procedure in the accelera tion–displacement response spectrum plane are illustrated in Fig. 24. The capacity curve of the equivalent SDOF system, transformed in a bilinear curve, is reported and the seismic demand corresponds to two values of the effective peak ground accelerations equal to $Sa_g = 0.1$ and $Sa_g = 0.2$ g; for the sake of clarity, only the elastic demand spectrum is shown. The seismic vulnerability is evaluated by comparing the displacement demand and the displacement capacity obtained through the pushover analyses. The displacement capacity and demand in the *X* and *Y* directions are then summarized for the towers under study in Figs. 25 and 26

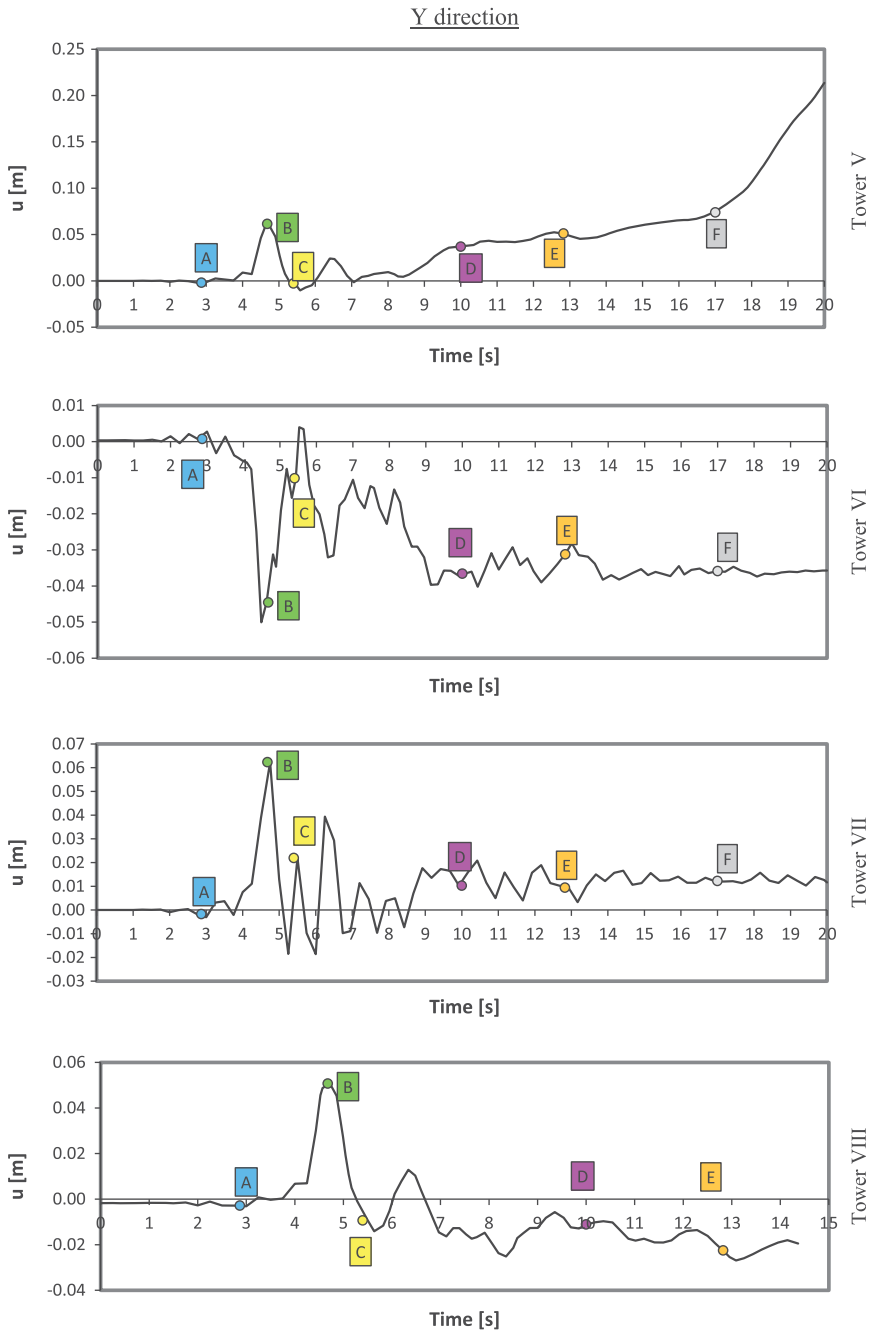

Fig. 17. Non-linear dynamic analyses, *Y* direction, PGA = 0.1 g. Displacement time history diagram for Towers V–VIII.

for two different seismic intensity levels. The results of the comparison of the two approaches in terms of displacement and safety verification are reported and discussed in detail for each tower.

- Tower I

According to the non-linear static procedure, Tower I is able to resist the seismic action corresponding to Sa_g = 0.1 g in the *X* and *Y* directions. This result is confirmed by the non-linear dynamic analyses. Moreover, the displacement demand obtained by the non-linear static procedure for both the directions is close to the maximum value of the top displacement experienced by the structure during the non-linear dynamic analysis. It can be also noted that the residual displacement obtained by the non-linear dynamic analyses is smaller than the structural capacity determined by the non-linear static procedure.

The application of the non-linear static procedure in the *X* direction shows that Tower I is not able to withstand the seismic action corresponding to Sa_g = 0.2 g and this result is supported by the non-linear dynamic analysis. The maximum value of the top displacement and the residual deformation obtained by the non-linear dynamic analysis are higher than the structural capacity determined by the non-linear static procedure. The maximum value of the top displacement found in the non-linear dynamic analysis is larger than the seismic demand obtained by the non-linear static procedure.

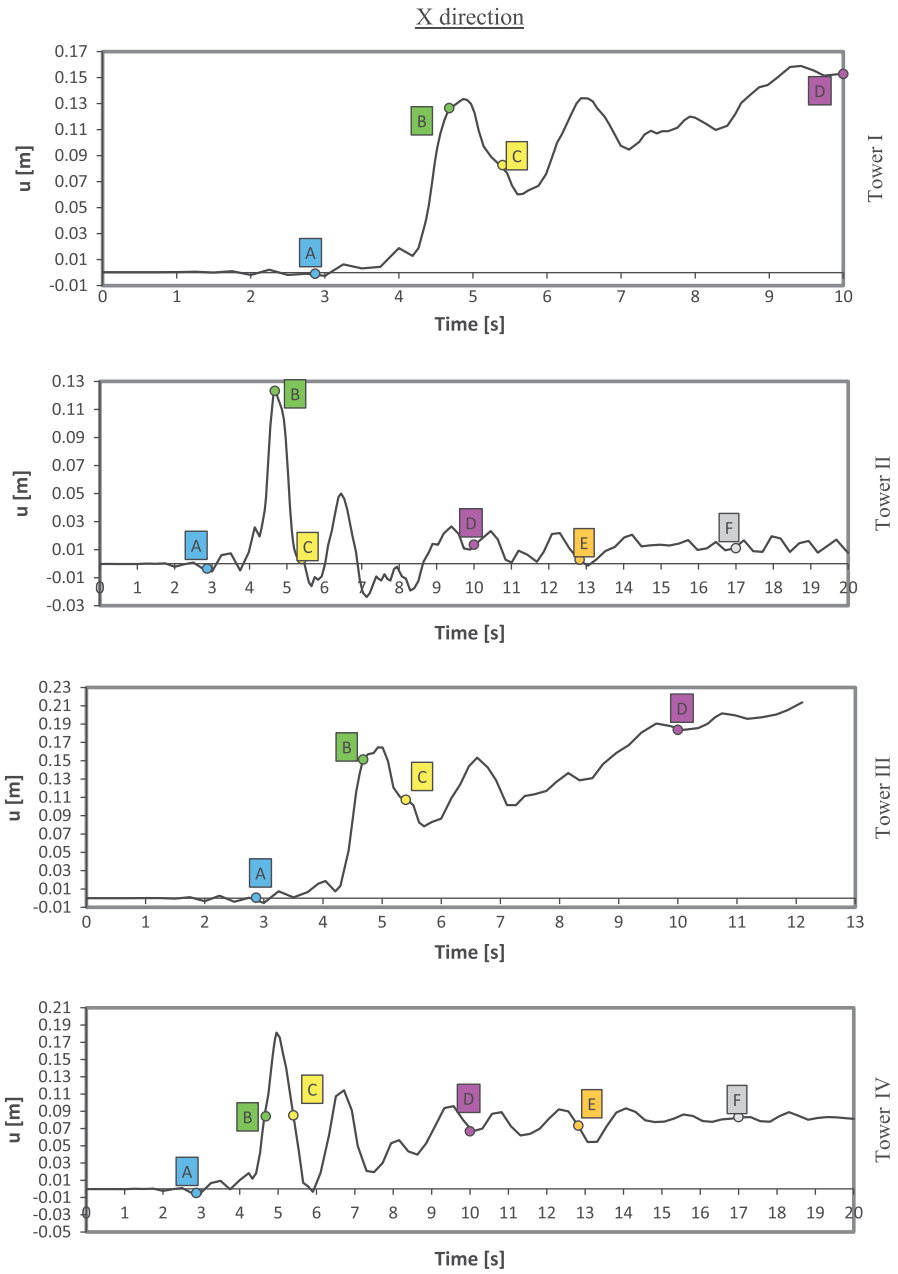

Fig. 18. Non-linear dynamic analyses, *X* direction, PGA = 0.2 g. Displacement time history diagram for Towers I–IV.

The application of the non-linear static procedure in the *Y* direction shows that Tower I is able to withstand the seismic action corresponding to $Sa_g = 0.2$ g. The maximum value of the top displacement obtained from the non-linear dynamic analysis is larger than the structural capacity obtained from the non-linear static procedure, but the value of the residual deformation at the end of the simulation is smaller than the capacity. The maximum value of the top displacement in the non-linear dynamic analysis is slightly larger than the seismic demand.

- Tower II

The theoretical predictions obtained from the non-linear static procedure show that Tower II is able to resist the seismic action corresponding to $Sa_g = 0.2$ g in the *X* and *Y* directions. This result is confirmed by the non-linear dynamic analyses. Moreover, the displacement demand obtained by the non-linear static procedure for both the directions is very close to the maximum value of the top displacement registered during the non-linear dynamic analyses. The residual displacement obtained by the non-linear dynamic analyses is smaller than the structural capacity determined by the non-linear static procedure.

- Tower III

According to the non-linear static procedure, Tower III is able to resist the seismic action corresponding to $Sa_g = 0.1$ g in the *X* and *Y* directions and this result is supported by the non-linear dynamic analyses. Moreover, the seismic demand obtained by the non-linear static procedure for both the directions is similar to the maximum value of the top displacement experienced by the structure during the non-linear dynamic analysis. The residual

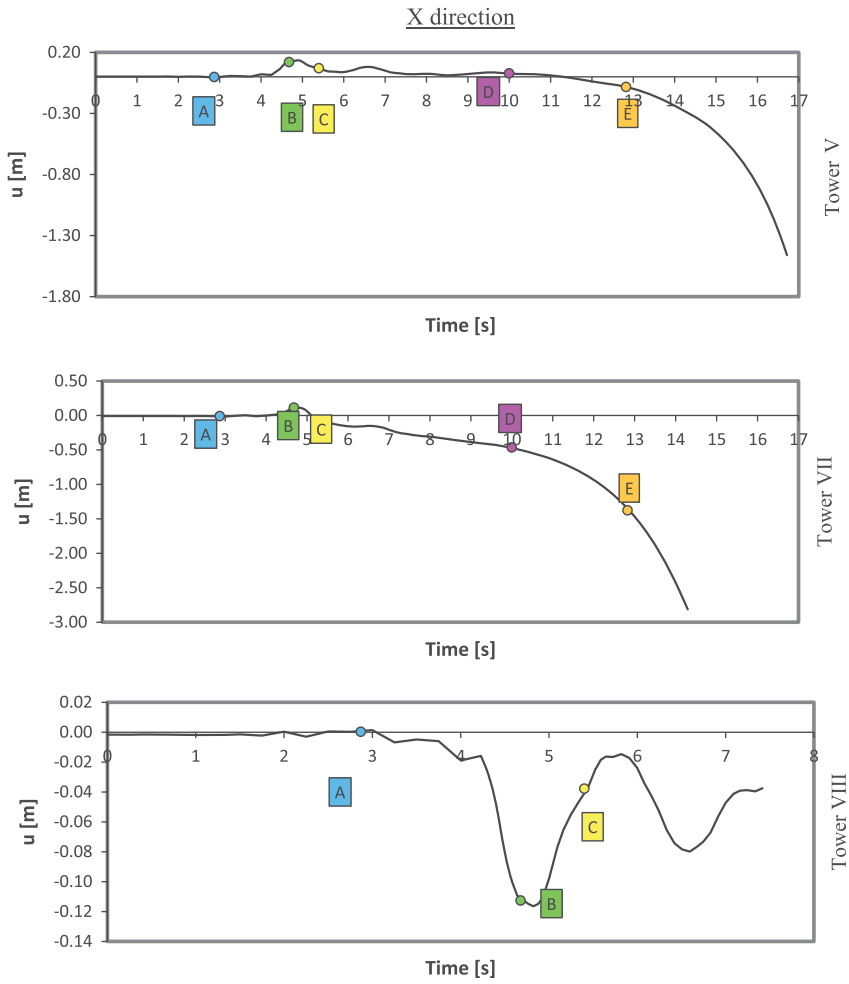

Fig. 19. Non-linear dynamic analyses, *X* direction, PGA = 0.2 g. Displacement time history diagram for Towers V, VII and VIII.

displacement obtained by the non-linear dynamic analyses is smaller than the structural capacity determined by the non-linear static procedure.

The application of the non-linear static procedure in the *X* direction shows that Tower III is not able to withstand the seismic action corresponding to $Sa_g = 0.2$ g. The corresponding non-linear dynamic analysis is not performed till the end and a possible collapse could not be definitely predicted. However, due to the large top displacements the structure can be considered as unsafe, which is in agreement with the results obtained by the non-linear static procedure. Moreover, the residual displacement obtained by the non-linear dynamic analysis is higher than the capacity of the structure determined by the non-linear static procedure.

The application of the non-linear static procedure in the *Y* direction shows that Tower III is not able to withstand the seismic action corresponding to $Sa_g = 0.2$ g. The maximum and residual displacements, obtained by the non-linear dynamic analysis, exceed the displacement capacity obtained from the non-linear static procedure. The seismic demand in the non-linear static procedure and the maximum value of the top displacement in the non-linear dynamic analysis are different, since the value of the displacement in the non-linear dynamic analysis is very large. The collapse mechanism is more evident in the *Y* direction.

- Tower IV

The theoretical predictions obtained from the non-linear static procedure show that Tower IV is able to resist the seismic action corresponding to $Sa_g = 0.2$ g in the *X* and *Y* directions and this result is supported by the non-linear dynamic analyses. Moreover, the displacement demand obtained by the non-linear static procedure for both the directions is very close to the maximum value of the top displacement registered during the non-linear dynamic analysis. The residual displacement obtained by the non-linear dynamic analyses is smaller than the structural capacity determined by the non-linear static procedure.

- Tower V

The application of the non-linear static procedure in the *X* direction shows that Tower V is not able to withstand the seismic action corresponding to $Sa_g = 0.2$ g and this result is supported by the non-linear dynamic analyses. Moreover, the displacement demand obtained by the non-linear static procedure in the *X* direction is smaller than the maximum value of the top displacement experienced by the structure during the non-linear dynamic analysis. The residual displacement obtained by the non-linear dynamic analyses is larger

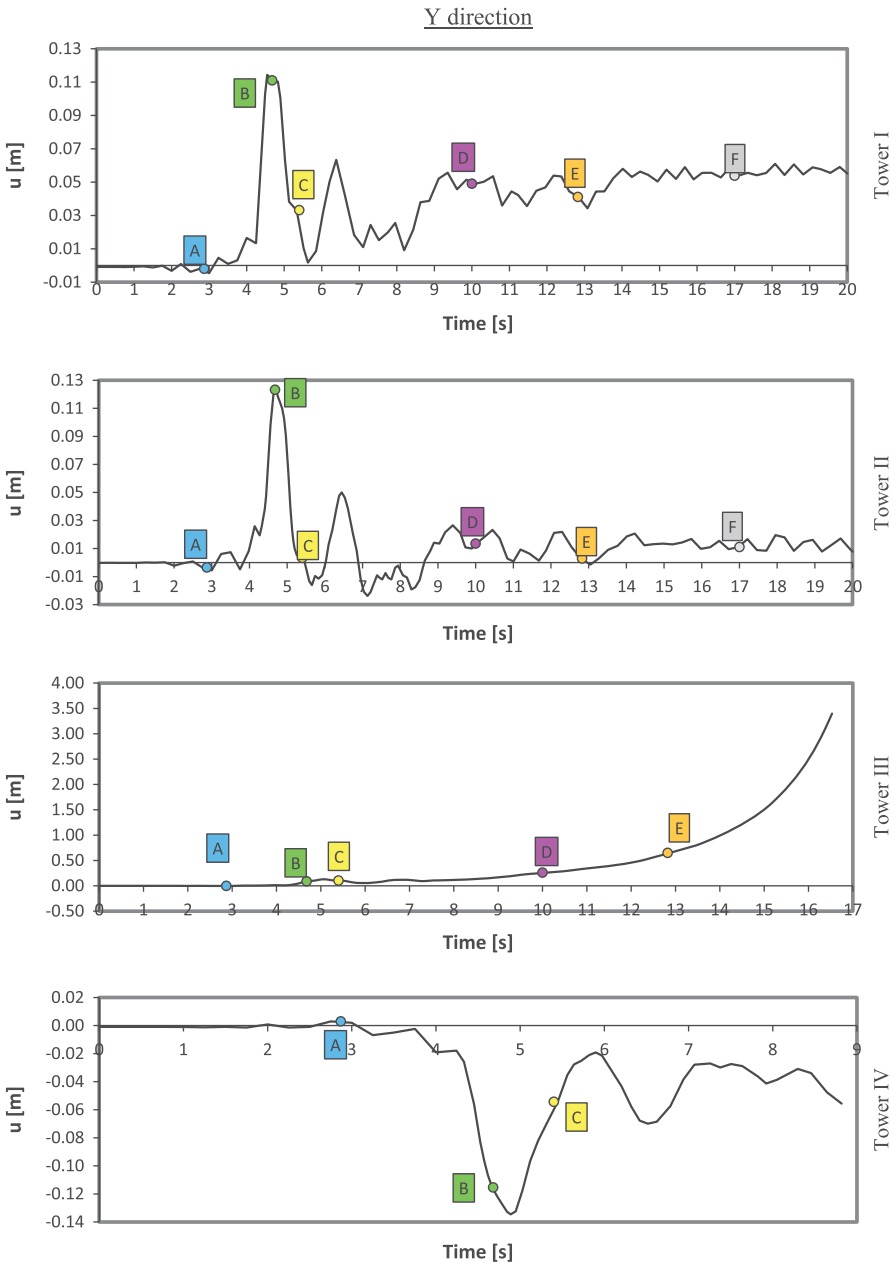

Fig. 20. Non-linear dynamic analyses, *Y* direction, PGA = 0.2 g. Displacement time history diagram for Towers I–IV.

than the structural capacity determined by the non-linear static procedure.

The application of the non-linear static procedure in the *Y* direction shows that Tower V is not able to withstand the seismic action corresponding to $Sa_g = 0.2$ g and this result is supported by the non-linear dynamic analyses. It can be noted that there is a large difference between the displacement demand obtained by the non-linear static procedure for $Sa_g = 0.1$ g and the maximum value of the top displacement registered during the non-linear dynamic analysis. The displacement demand computed by the non-linear static procedure is smaller than the capacity of the structure, while a local collapse involving the internal vaults is clearly indicated by the non-linear dynamic analysis.

- Tower VI

The behavior of Tower VI is significantly affected by the presence of the weak wall with small thickness characterized by a large opening at the top. The results are different in function of the control point under consideration.

If the corner node of the strong wall is selected as a control point, the theoretical predictions obtained from the non-linear static procedure show that Tower VI is able to resist the seismic action corresponding to $Sa_g = 0.1$ g in the *X* direction. Moreover, the maximum value of the top displacement experienced by the structure during the non-linear dynamic analysis is close to the seismic demand and the residual displacement is smaller than the capacity, which indicates that the structure is safe. This is due to the fact

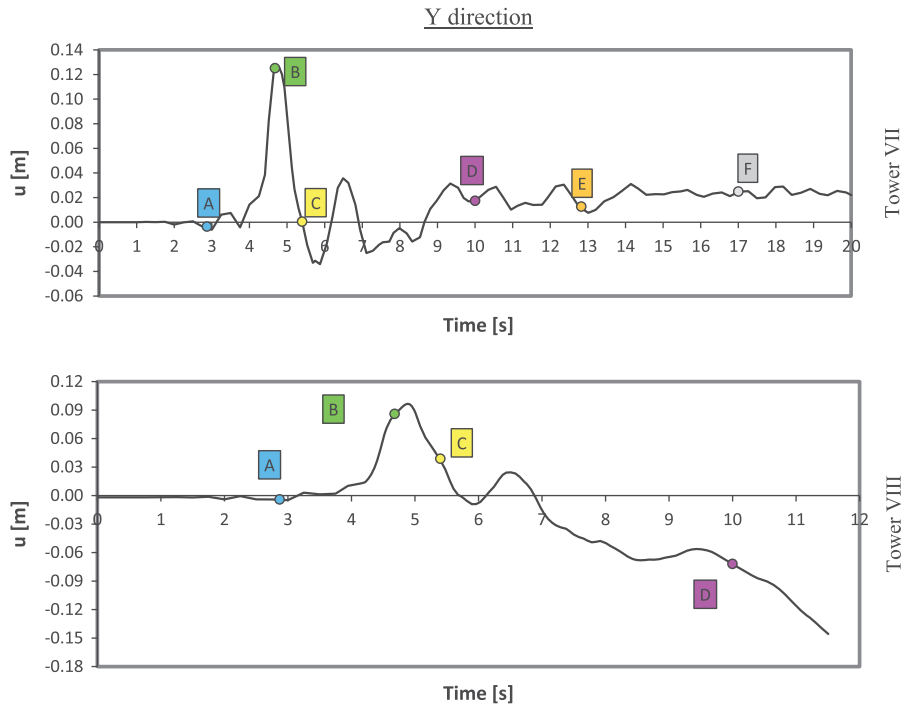

Fig. 21. Non-linear dynamic analyses, *Y* direction, PGA = 0.2 g. Displacement time history diagram for Towers VII and VIII.

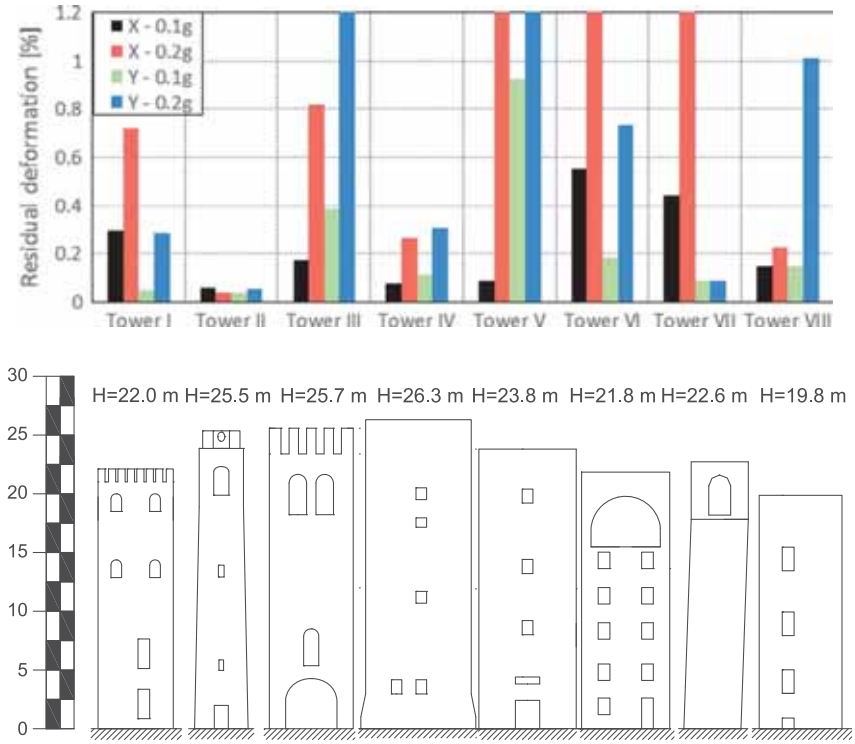

Fig. 22. Non-linear dynamic analyses: residual deformations at PGA = 0.1 g and PGA = 0.2 g in the *X* and *Y* directions for the different towers.

that this control node is not part of the weak wall of the tower that experiences large displacements. This control node could be used in the non-linear static procedure to represent the global behavior of the tower, but it can't clearly detect local failure mechanisms.

On the contrary, if the corner node of the weak wall is chosen as a control point, the results are different. Maximum and residual displacements obtained by the non-linear dynamic analysis exceed the structural capacity obtained by the non-linear static procedure and the tower can't be considered as safe. In fact, when the structure is subjected to loading in the *X* direction, the weak wall deforms easily and moves in a different way compared to the other wall in the same direction, which is much stiffer. In this case, the capacity of the building is underestimated, since the results refer to the weak part of the tower. Consequently, for plan-wise

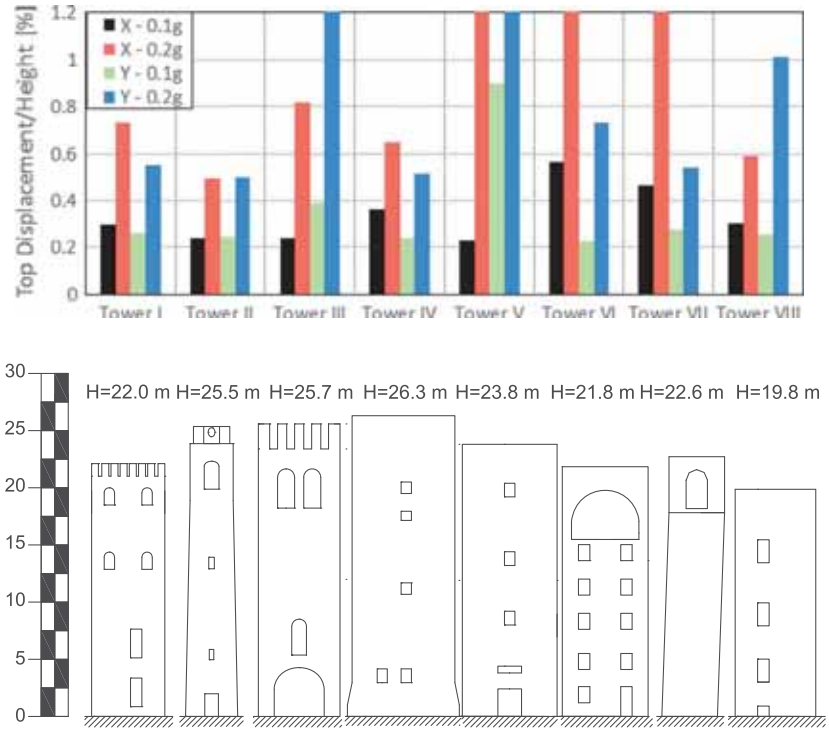

Fig. 23. Non-linear dynamic analyses: maximum normalized top displacement (top displacement/height) at PGA = 0.1 g and PGA = 0.2 g in the *X* and *Y* directions for the different towers (values of normalized top displacements are interrupted at 1.2%).

irregular towers, more than one control point should be used as an indicator of the structural behavior and the results have to be evaluated with caution.

- Tower VII

The application of the non-linear static procedure in the *Y* direction shows that Tower VII is able to withstand the seismic action corresponding to $Sa_g = 0.1$ g, while the structure is at the critical point for $Sa_g = 0.2$ g. The displacement demand obtained by the non-linear static procedure is very similar to the maximum value of the top displacement registered during the non-linear dynamic analysis. The residual displacements obtained by the non-linear dynamic analyses are smaller than the structural capacity determined by the non-linear static procedure, which may prove that there is no collapse of the structure.

The behavior of the tower is affected by the quite relevant inclination in the negative *X* direction. According to the non-linear static procedure, Tower VII is not able to resist the seismic action corresponding to $Sa_g = 0.2$ g in the *X* direction, which is in agreement with the results from the non-linear dynamic analyses. However, the comparison between the two methods in terms of displacements indicates that the seismic demands (0.1 g and 0.2 g) do not correspond to the maximum value of the top displacements registered during the non-linear dynamic analyses. The possible collapse mechanism is the detachment of one of the walls in the *Y* direction.

- Tower VIII

The theoretical predictions obtained from the non-linear static procedure show that Tower VIII is able to resist the seismic action corresponding to $Sa_g = 0.1$ g in the *X* and *Y* directions. The maximum values of the top displacements experienced by the structure during the non-linear dynamic analyses are close to the ones obtained from the non-linear static procedure.

The application of the non-linear static procedure in the *Y* direction shows that Tower VIII is not able to withstand the seismic action corresponding to $Sa_g = 0.2$ g; on the contrary, the displacement demand and capacity are very similar in the *X* direction. It can be noted that a local collapse of the slab at the top of the tower is shown by the non-linear dynamic simulations. Such a local collapse is not captured by the pushover analysis.

The results obtained from the non-linear static procedure are also synoptically summarized in Table 2 for a direct comparison with the outcomes of the non-linear dynamic analyses. As can be noted, the seismic safety assessment provided by the two methods is very similar for almost all the towers, in some cases with a very satisfactory agreement. The non-linear static procedure may provide reasonable synthetic predictions of the seismic vulnerability of the towers. A slightly more conservative trend for the non-linear dynamic simulations can be noticed after a detailed analysis of individual cases. The non-linear static procedure provides smaller values of displacement demand than those resulting from the non-linear dynamic analyses. The simplified static approach is not able to capture the inertial effects associated with seismic excitation that can lead to heavy damage and premature collapse of the structure.

7. Damage contour plots

The agreement between the non-linear dynamic and non-linear static approaches is finally verified by the damage contour plots obtained at the end of the numerical simulations and reported from Figs. 27–34. The same trend of damage is generally noted for the two approaches in the majority of the towers, with, in some

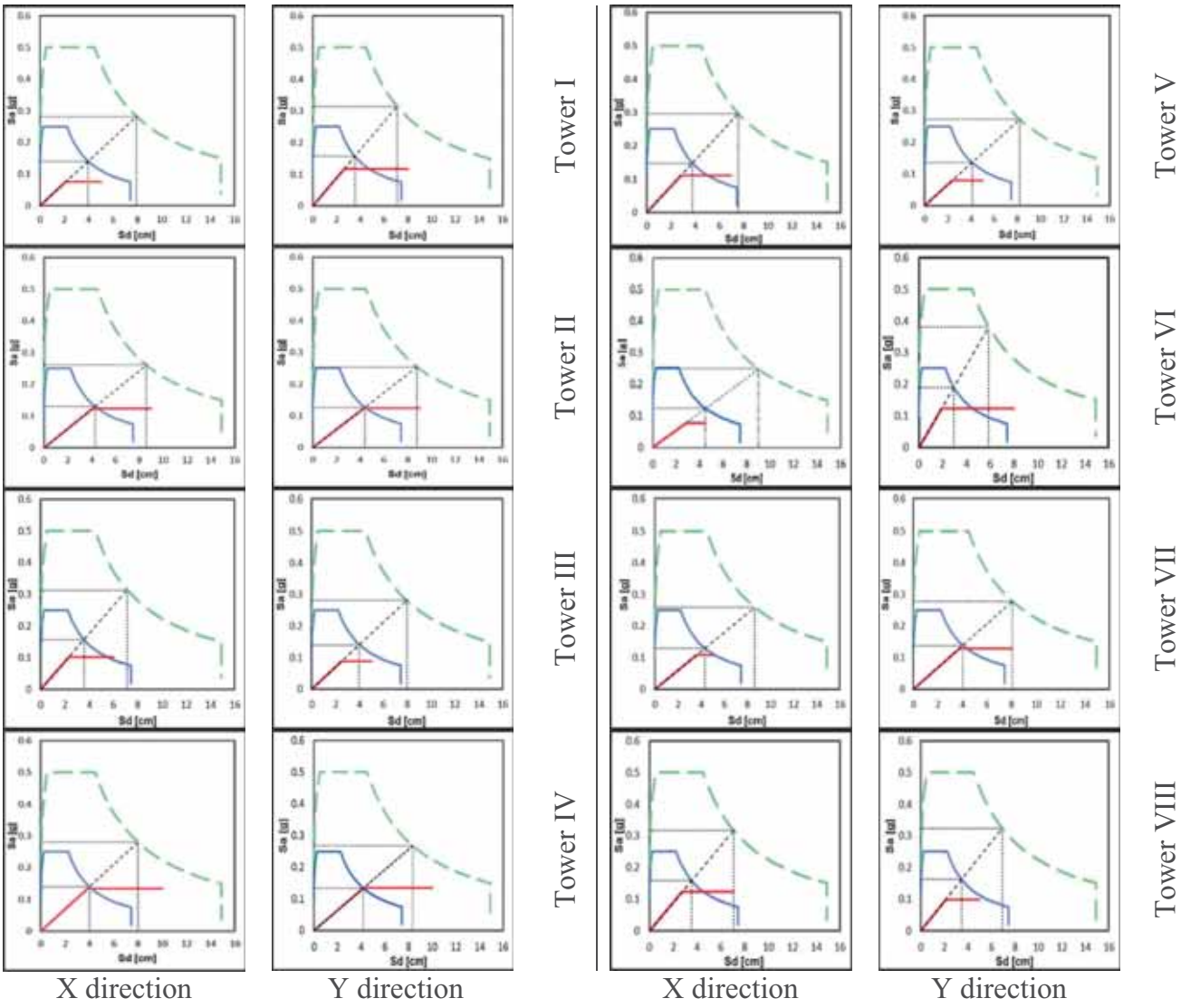

Fig. 24. Non-linear static procedure in the acceleration–displacement response spectrum plane (*X* and *Y* directions) for different seismic intensity levels: $Sa_g = 0.1$ g (continuous blue line) and $Sa_g = 0.2$ g (dashed green line). (For interpretation of the references to color in this figure legend, the reader is referred to the web version of this article.)

cases, typical damage spreading along vertical lines, as usually observed for slender towers with regularly distributed perforations in the absence of internal cross vaults. Different geometrical characteristics of the towers result into complex and different damage patterns under horizontal loads.

- Tower I

Severe damage is mainly concentrated near the openings along the whole height of the walls in the *X* direction, see Fig. 27. Similar damage distributions are obtained by the non-linear static procedure and at the end of the non-linear dynamic analysis, but numerical values are smaller in the non-linear static procedure. In addition, a damage concentration is observed at the base of the tower in the pushover analysis. Since *X* is the weakest direction of the structure, damage on the walls in the *X* direction is present independently from the direction of the seismic action, while the walls in the *Y* direction are damaged only when the seismic action is applied in the same direction.

- Tower II

A clear damage distribution for vertical shear along the whole height of the tower is registered on all the walls, see Fig. 28. Damage propagates vertically and concentrates along the openings in the bell cell. The damage distribution obtained by the non-linear static procedure is similar to the one observed at the end of the non-linear dynamic analyses, but it is less evident.

- Tower III

Non-linear dynamic analyses performed under PGA = 0.2 g indicate widespread damage distributed on all the walls of the tower, see Fig. 29. An extensive damage, with the probable occurrence of an active failure mechanism, is registered mainly in the case of application of the seismic action in the *Y* direction. Damage is rather evident immediately over the large opening at the base. The upper part of the tower presents wide openings and slender perimeter walls; it is severely damaged in both the numerical

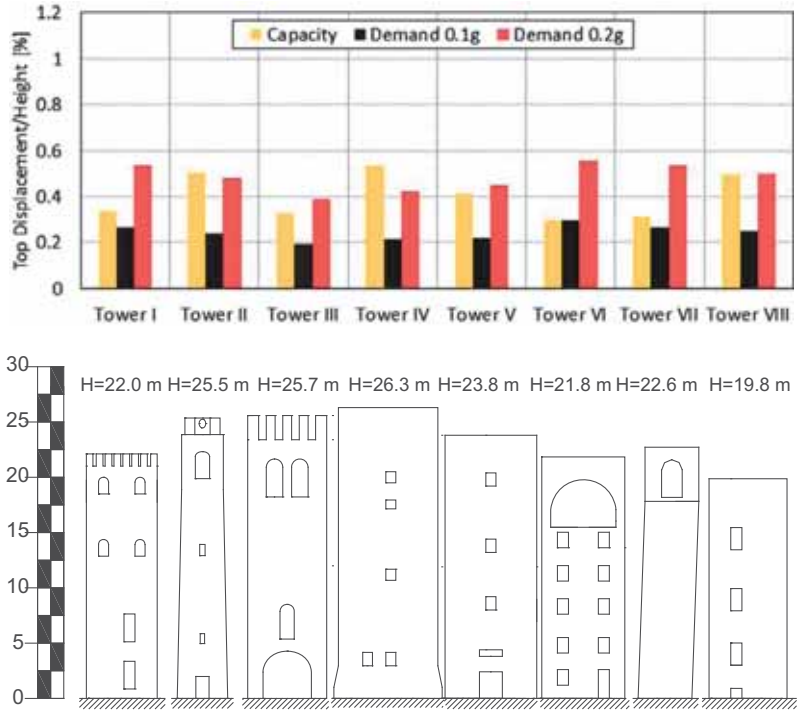

Fig. 25. Non-linear static procedure, *X* direction: displacement capacity and displacement demand at different seismic intensity levels for the different towers.

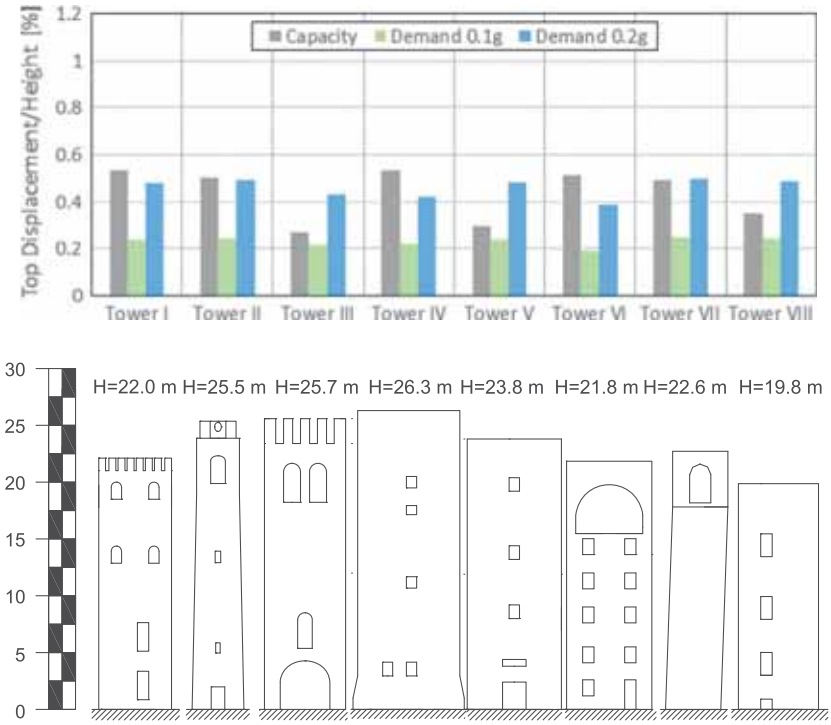

Fig. 26. Non-linear static procedure, *Y* direction: displacement capacity and displacement demand at different seismic intensity levels for the different towers.

approaches. The values of damage corresponding to the displacement demand found by the non-linear static procedure are much smaller than those at the end of the dynamic simulations, because different displacements are reached. However, the non-linear static procedure gives a good approximation of the damage pattern and indicates the vulnerable parts of the structure.

- Tower IV

A clear damage for vertical shear is observed along the whole height of the tower, see Fig. 30. In the dynamic simulations with PGA = 0.1 g damage is less visible but already present. The distribution of damage corresponding to the displacement demand of the

Table 2
Comparison on the collapse state of the towers evaluated through the non-linear static procedure and the non-linear dynamic analyses: *X* and *Y* directions, PGA = 0.1 g and PGA = 0.2 g.

Collapse √YES × NO √/× Borderline	*X* direction				*Y* direction			
	Non-linear static procedure		Non-linear dynamic analysis		Non-linear static procedure		Non-linear dynamic analysis	
Tower	PGA 0.1 g	PGA 0.2 g	PGA 0.1 g	PGA 0.2 g	PGA 0.1 g	PGA 0.2 g	PGA 0.1 g	PGA 0.2 g
I	×	√	×/√	√	×	×	×	×/√
II	×	×	×	×	×	×/√	×	×
III	×	√	×	√	×	√	×/√	√
IV	×	×	×	×/√	×	×	×	×/√
V	×	√	×	√	×	√	√	√
VI	×/√	√	√	√	×	×	×	√
VII	×	√	×/√	√	×	×/√	×	×
VIII	×	×/√	×/√	×/√	×	√	×	√

non-linear static procedure is similar to the one observed during the non-linear dynamic analysis. The damage pattern is affected by the presence of small openings and it propagates along vertical lines.

- Tower V

A severe and widespread damage may be noticed by looking at the image of the tower at the end of the dynamic simulations with PGA = 0.2 g in the *X* direction, see Fig. 31. In particular, a damage concentration in the upper part of the tower and near the internal masonry vaults may be observed. The possible occurrence of an active failure mechanism seems clear. In pushover analyses an inclined pattern of damage is clearly visible; in non-linear dynamic analyses damage is vertically distributed along the height of the tower. A localized damage as a result of a redistribution of internal actions transferred by the vaults is registered mainly in the dynamic simulations.

- Tower VI

Damage contour plot is reported for both the analyses under PGA = 0.1 g. It is clear that severe damage is concentrated in the front wall characterized by small thickness and multiple openings for both the analyses and for both the directions of the seismic action, see Fig. 32. Non-linear dynamic analyses highlight a potential failure mechanism represented by the detachment of the front wall. Both the analyses show large damage propagating on the back wall too. A considerable damage is clearly visible at the top of the tower above the big opening of the front wall, indicating a probable partial collapse of the most vulnerable part of the structure.

- Tower VII

A severe and widespread damage is evident on all the walls by looking at the image of the tower at the end of the dynamic simulations with PGA = 0.2 g in the *X* direction, see Fig. 33. A possible failure mechanism can be deduced. The damage corresponding to the displacement demand found by the non-linear static procedure is much smaller and less diffused than the one at the end of the dynamic simulations, because different displacements are reached. In the pushover analysis in the *X* direction damage spreads in a limited portion of the tower near the base. In the *Y* direction the damage distributions are similar for the two approaches, but damage is less evident in the pushover analysis. From the dynamic simulations performed, it can be deduced that the inclination makes the structure quite vulnerable to damage.

- Tower VIII

The damage distribution obtained by the two methods is similar and it is concentrated mainly near the openings along the whole height of the walls, see Fig. 34. Clear diffused vertical damage is mainly observed on the walls in the *Y* direction for both the analyses under PGA = 0.2 g. The walls in the *Y* direction are completely damaged and the occurrence of an active failure mechanism is possible. A damage distribution under seismic excitation is quite diffused, but presents some relevant peaks near the openings.

8. Discussion of results

8.1. Comparison between the procedures

The displacement demands obtained by the non-linear static procedure are in a good agreement with those obtained by the non-linear dynamic analyses when the check of the structural safety is verified. When the check is not satisfied according to the non-linear static procedure, the seismic demand is smaller than the maximum value of the top displacement experienced by the structure during the non-linear dynamic analyses. In the majority of cases this result can be explained by the large increase of the displacements registered in the non-linear dynamic analyses when a collapse mechanism occurs. From an overall analysis of the results, it can be noted that the non-linear static procedure generally gives reliable results in terms of displacements. Large differences are observed in the cases of Tower V and Tower VI, where local collapse mechanisms are registered during the non-linear dynamic analyses and for this reason the displacement distribution differs significantly. In the case study of Tower V, the non-linear static procedure does not catch the collapse of the upper vaults, which is registered at the end of the non-linear dynamic analyses. In the case study of Tower VI, a local collapse of the upper part of the thin wall is clearly observed during the non-linear dynamic analysis: moreover the presence of this type of irregularity triggers non-uniform displacement demands at the top of the structure. Non-linear dynamic analyses are able to account for higher mode effects that may be introduced by local irregularities.

The tensile damage distribution corresponding to the displacement demand is generally similar to the damage pattern observed at the end of the non-linear dynamic analyses, but the numerical

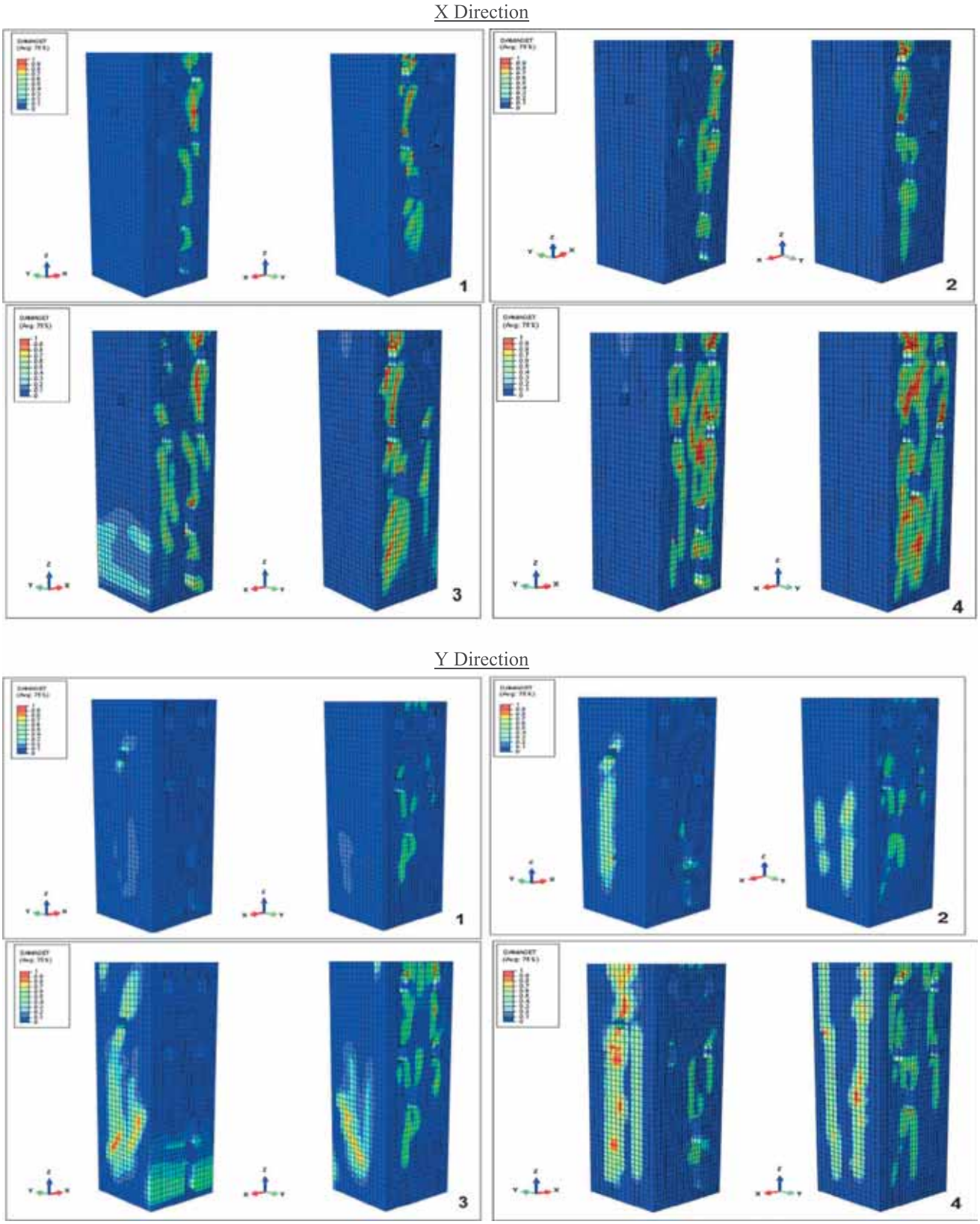

Fig. 27. Tower I. Comparison between the damage contour plots obtained through the non-linear static procedure (1 and 3) and the non-linear dynamic analysis (2 and 4). 1 and 2: PGA = 0.1 g. 3 and 4: PGA = 0.2 g.

values of damage are always smaller. The only exception is the severe damage observed at the base of the towers during the pushover analyses: it is less evident at the end of the non-linear dynamic analyses. However, the damage pattern detected by the pushover analysis can represent a good indicator of the vulnerable parts of the structure.

Fig. 28. Tower II. Comparison between the damage contour plots obtained through the non-linear static procedure (1 and 3) and the non-linear dynamic analysis (2 and 4). 1 and 2: PGA = 0.1 g. 3 and 4: PGA = 0.2 g.

The choice of the control point, representative of the global behavior of the structure, is a fundamental issue for the application of the non-linear static procedure. The results of the procedure significantly depend on the selection of the control point and, in some cases, show quite large variations. Therefore, the results obtained by the non-linear static procedure should be evaluated with caution in function of the control point chosen for the procedure. This result is proven by the study of the Tower VI, where torsional effects are evident. It is shown that the results obtained with a control point which is not part of the local collapse overestimate the capacity of the structure. On the contrary, if a point belonging to the vulnerable part of the structure is chosen as a control point, the results underestimate the capacity of the structure.

The non-linear static procedure can give a satisfactory representation of the seismic behavior of the towers in terms of structural safety verification and displacement demands when

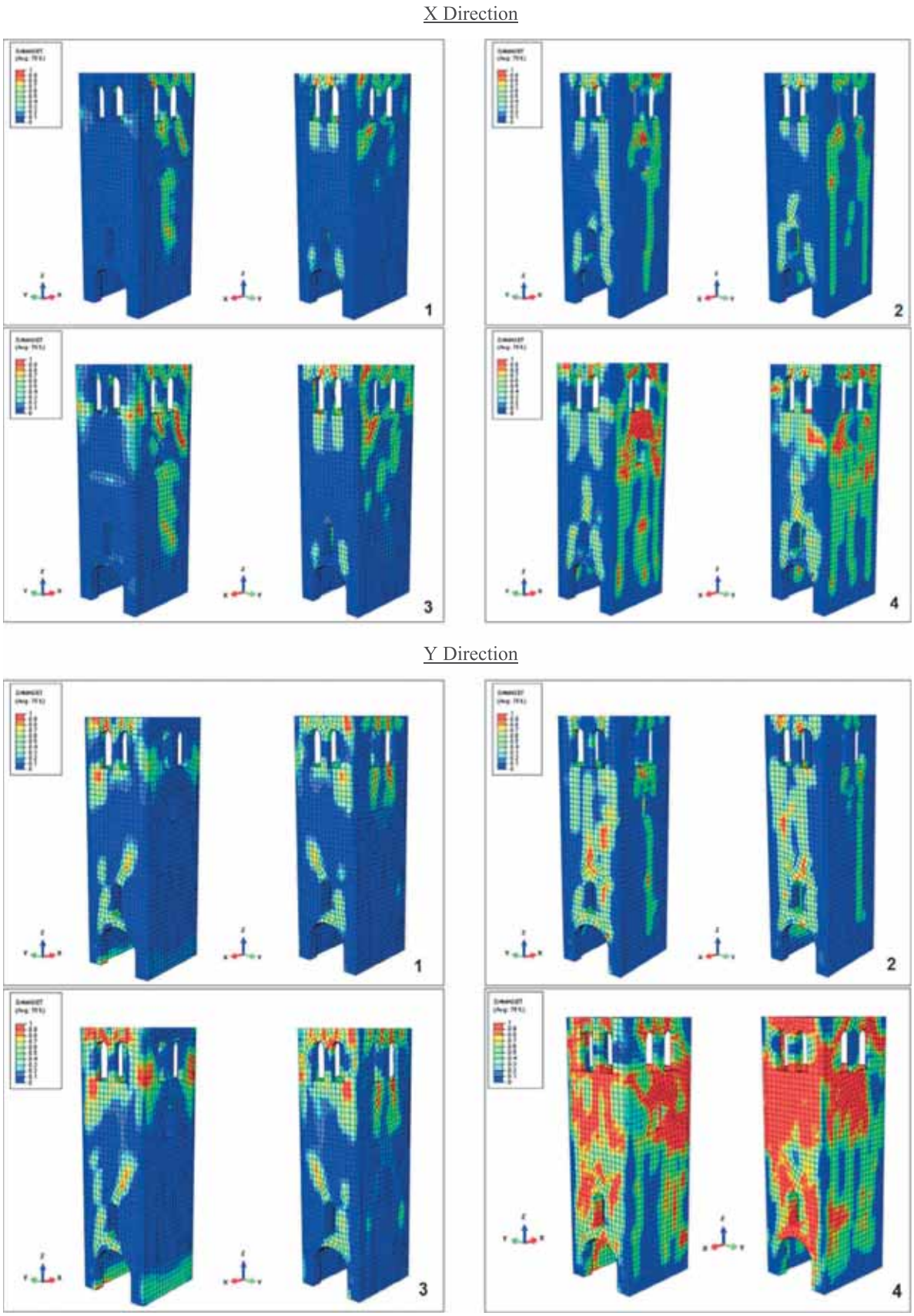

Fig. 29. Tower III. Comparison between the damage contour plots obtained through the non-linear static procedure (1 and 3) and the non-linear dynamic analysis (2 and 4). 1 and 2: PGA = 0.1 g. 3 and 4: PGA = 0.2 g.

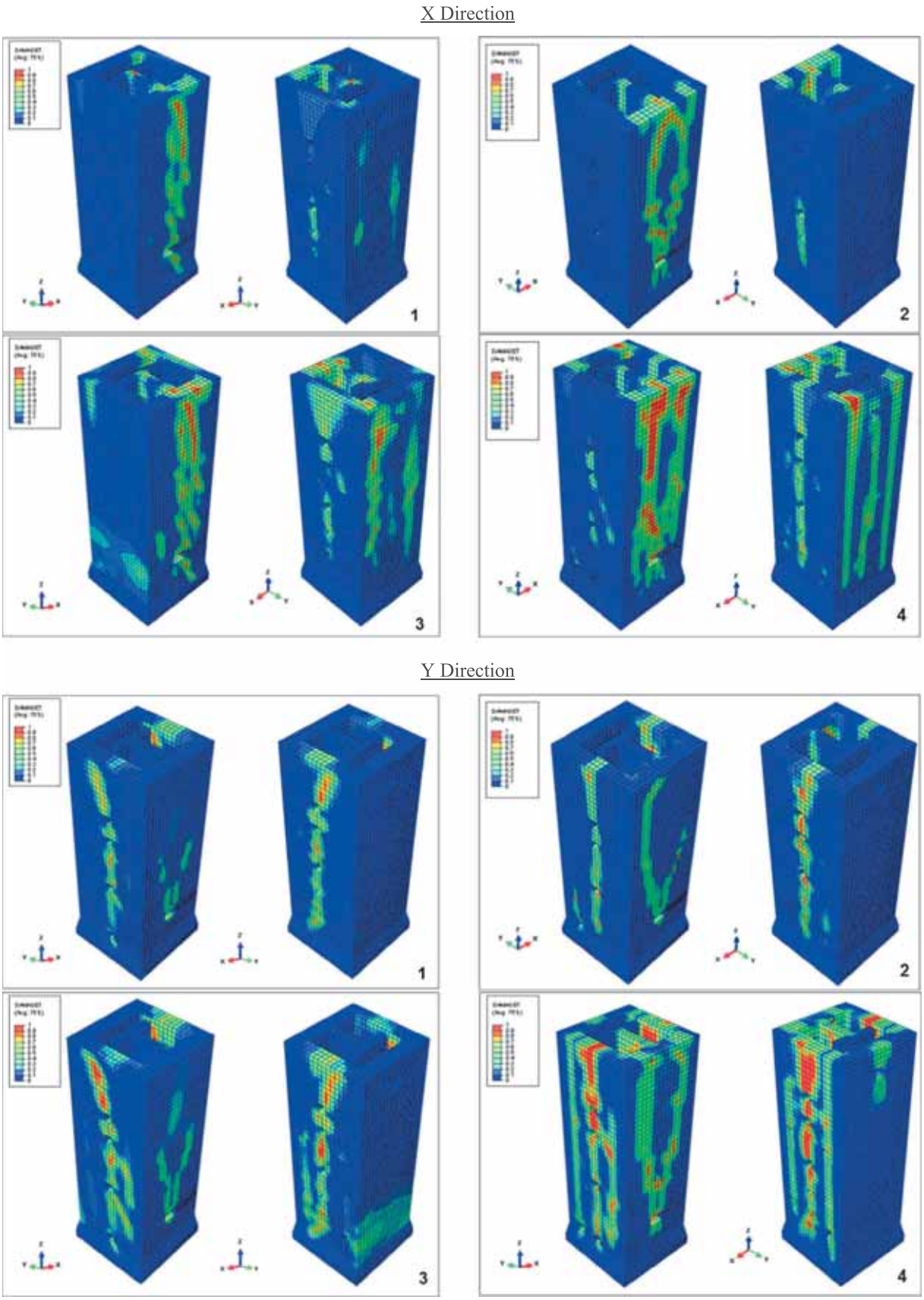

Fig. 30. Tower IV. Comparison between the damage contour plots obtained through the non-linear static procedure (1 and 3) and the non-linear dynamic analysis (2 and 4). 1 and 2: PGA = 0.1 g. 3 and 4: PGA = 0.2 g.

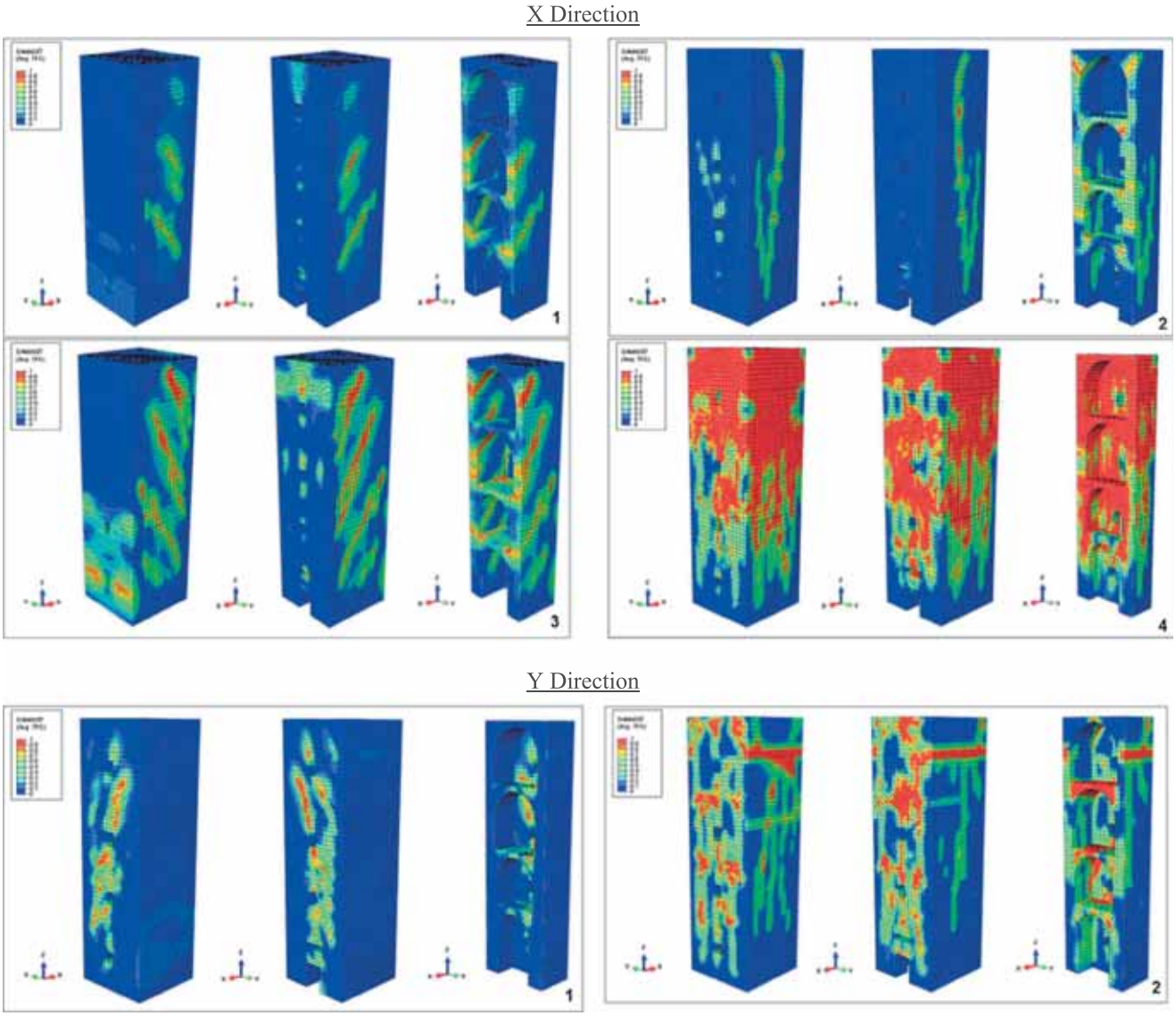

Fig. 31. Tower V. Comparison between the damage contour plots obtained through the non-linear static procedure (1 and 3) and the non-linear dynamic analysis (2 and 4). 1 and 2: PGA = 0.1 g. 3 and 4: PGA = 0.2 g.

significant irregularities are not present. In slender towers with presence of irregularities the contribution of higher modes to the global response may be considerable. Structures with higher mode effects exhibit a complex dynamic response that necessitates the use of more sophisticated methods of analyses.

8.2. Seismic safety assessment and failure modes of the towers

The check of the seismic safety of the analyzed towers is satisfied according to the non-linear static procedure under Sa_g = 0.1 g, with the exception of Tower VI that is a borderline case. Similar results are obtained through the non-linear dynamic analyses. Only Tower V and Tower VI present large residual deformations, indicating the activation of local failure mechanisms, mainly due to the geometrical irregularities, even for peak ground acceleration equal to 0.1 g.

According to the non-linear static procedure, the analyzed towers are not able to accommodate the seismic demand under Sa_g = 0.2 g, with the exception of Tower IV and Tower II. These results are supported by the outcomes of the non-linear dynamic analyses.

The peculiar geometrical characteristics and configurations are the main reasons of the larger seismic resistance of these two towers than the one of the other towers. In the case of Tower IV, the thickness of the four perimeter walls is larger than the one of the other towers and it remains constant along the height of the structure. In addition, at the top of the tower there are no large openings, which can represent a vulnerable upper part, when compared to the majority of the other towers. Tower II is symmetrical both in plan and in elevation and presents a regular internal distribution. The tower has a square plan and its weight is much smaller than the one of the other towers, leading to a great reduction of the seismic forces.

For the other towers under study, different failure modes can be observed. The role played by both the geometrical characteristics and the presence of irregularities on the possible collapse mechanisms is highlighted by the results of the analyses. Problems relative to the structural configuration, especially asymmetry and inadequate arrangement of openings, can affect the level of damage in the towers.

A non-uniform stiffness and strength distribution, in plan and elevation, and torsional effects can be some of the main causes for a widespread damage and even collapse of the towers. Tower

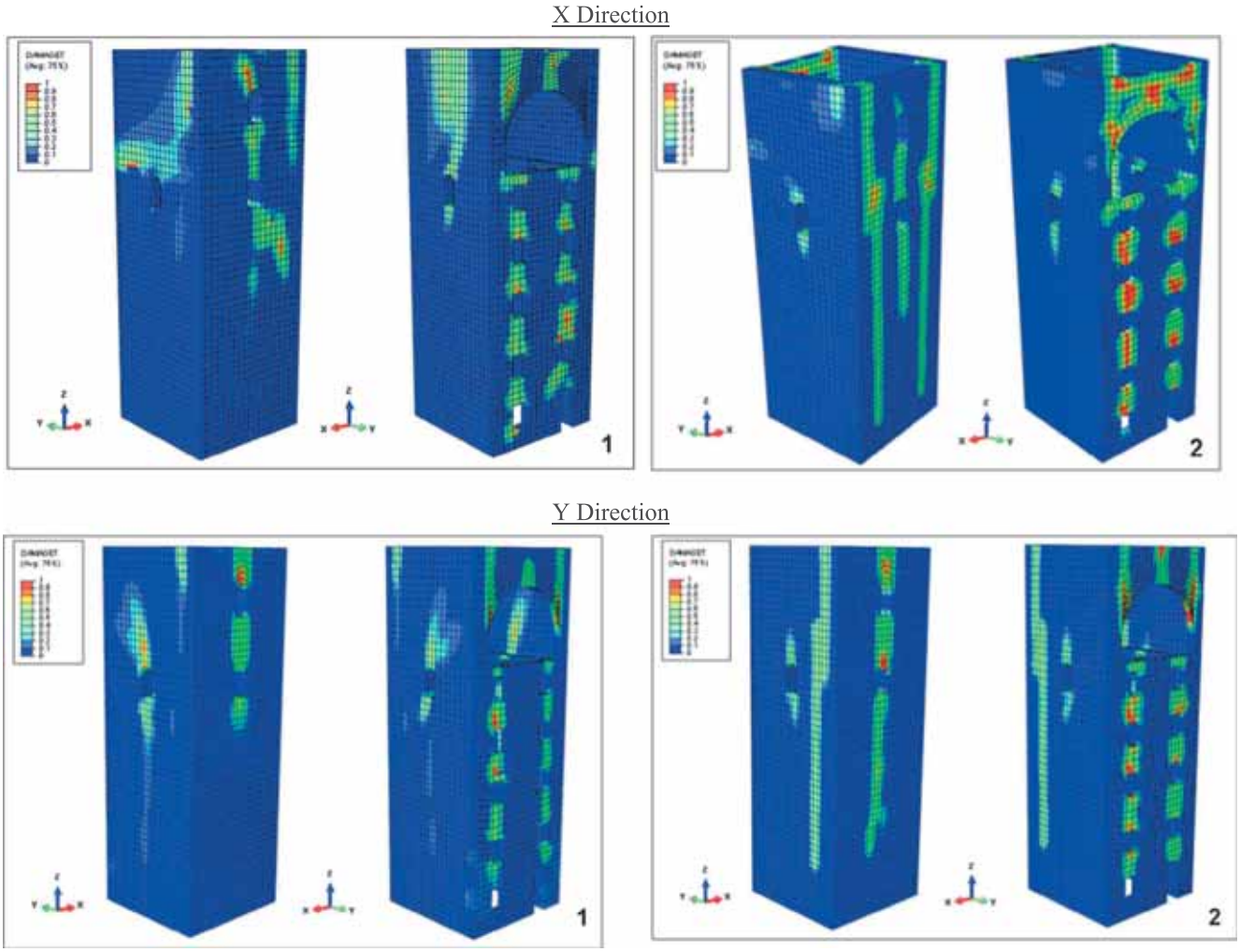

Fig. 32. Tower VI. Comparison between the damage contour plots obtained through the non-linear static procedure (1) and the non-linear dynamic analysis (2). PGA = 0.1 g.

VI is characterized by a wall with small thickness and a large opening at the top. A failure mechanism involving the detachment of the wall is registered.

For Tower V and Tower VIII, the role played by the internal vaults in modifying the load path for gravity and earthquake loads is evident and unexpected stress concentrations may arise. Localized and severe damage as a result of a redistribution of internal actions transferred by the vaults is highlighted by the analyses. Moreover, Tower V exhibits sudden variations of the walls thickness along the height and Tower VIII presents some irregularities within the perimeter walls.

The quite marked inclination, the high slenderness and the plan asymmetry are the main causes for the widespread damage of Tower VII.

A significant reduction of stiffness and strength of a wall is observed when multiple openings are present, like in the cases of Tower I and Tower III. Tower I has several openings on two parallel walls and Tower III presents large openings both at the base and at the top. A damage concentration with cracks propagating vertically is observed near the openings.

9. Conclusions

A comprehensive numerical study conducted by means of advanced FE simulations (non-linear dynamic and static analyses) on eight historical masonry towers located in the North-East region of Italy is presented. The main aims of this work are the following: (1) to point out some general effects of the morphological and geometrical characteristics, such as openings, wall thickness and irregularities, on the seismic performance of the towers, by using detailed 3D FE models; (2) to assess the seismic safety of the towers by non-linear dynamic and static analyses; (3) to compare the results of the two different approaches in order to evaluate the effectiveness of the non-linear static procedure.

From an overall analysis of the results obtained in this study, the following conclusions may be drawn.

- The results of the non-linear dynamic simulations show the high vulnerability of historical masonry towers under horizontal loads. It can be roughly stated that if a residual deformation ranging between 0.4% and 0.8% is reached, the structure may be reasonably considered near collapse.
- Some geometrical characteristics, such as plan and elevation irregularities, presence of belfry, large openings, sudden variation of cross-section, internal vaults and tower inclination, play a crucial role on the seismic performance of the towers. The correlation between local geometrical issues and possible failure modes of the towers is clearly highlighted by the numerical analyses.
- From some considerations on the residual deformations obtained from the non-linear dynamic analyses and theoretical predictions provided by the non-linear static procedure, an

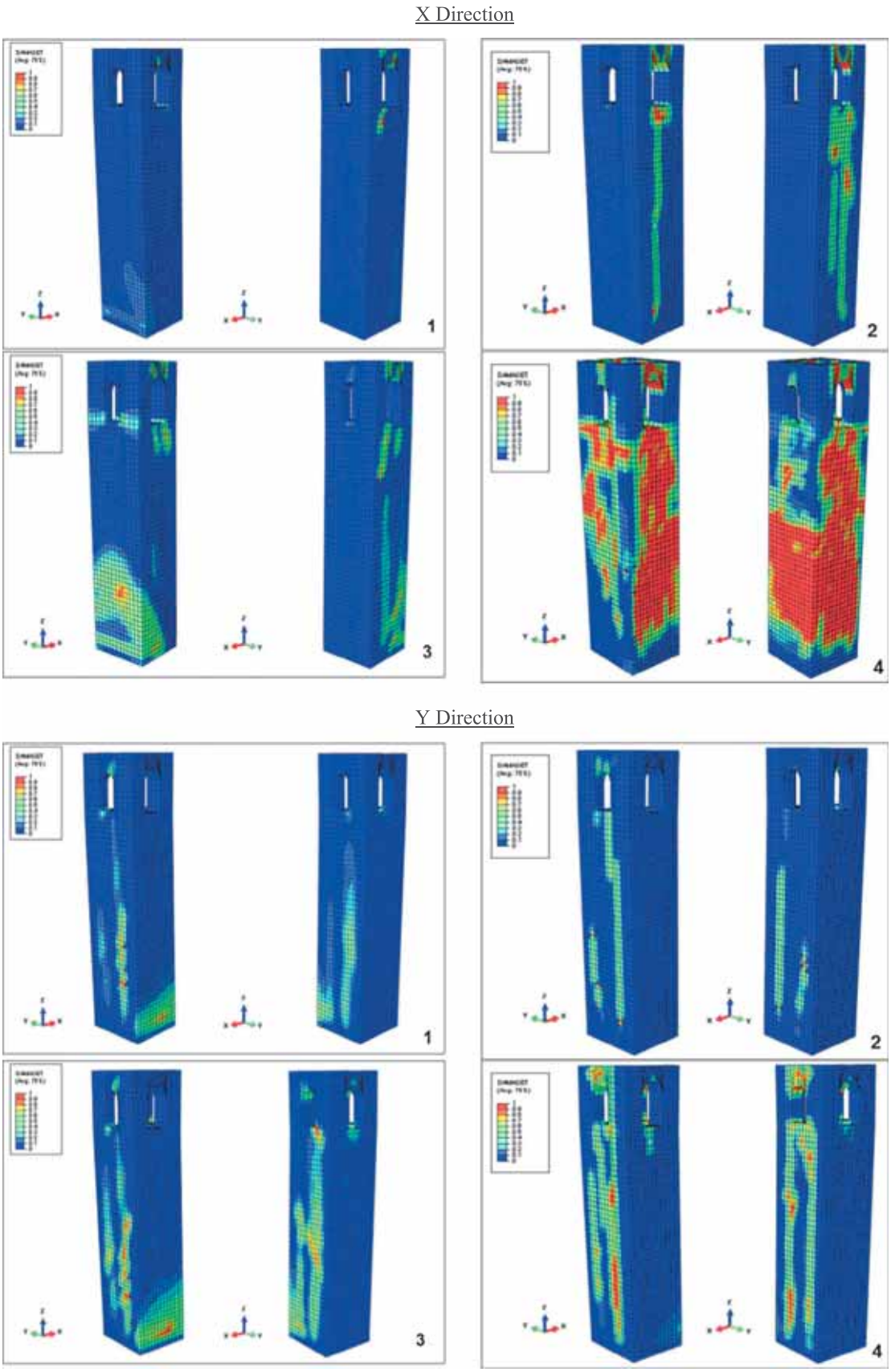

Fig. 33. Tower VII. Comparison between the damage contour plots obtained through the non-linear static procedure (1 and 3) and the non-linear dynamic analysis (2 and 4). 1 and 2: PGA = 0.1 g. 3 and 4: PGA = 0.2 g.

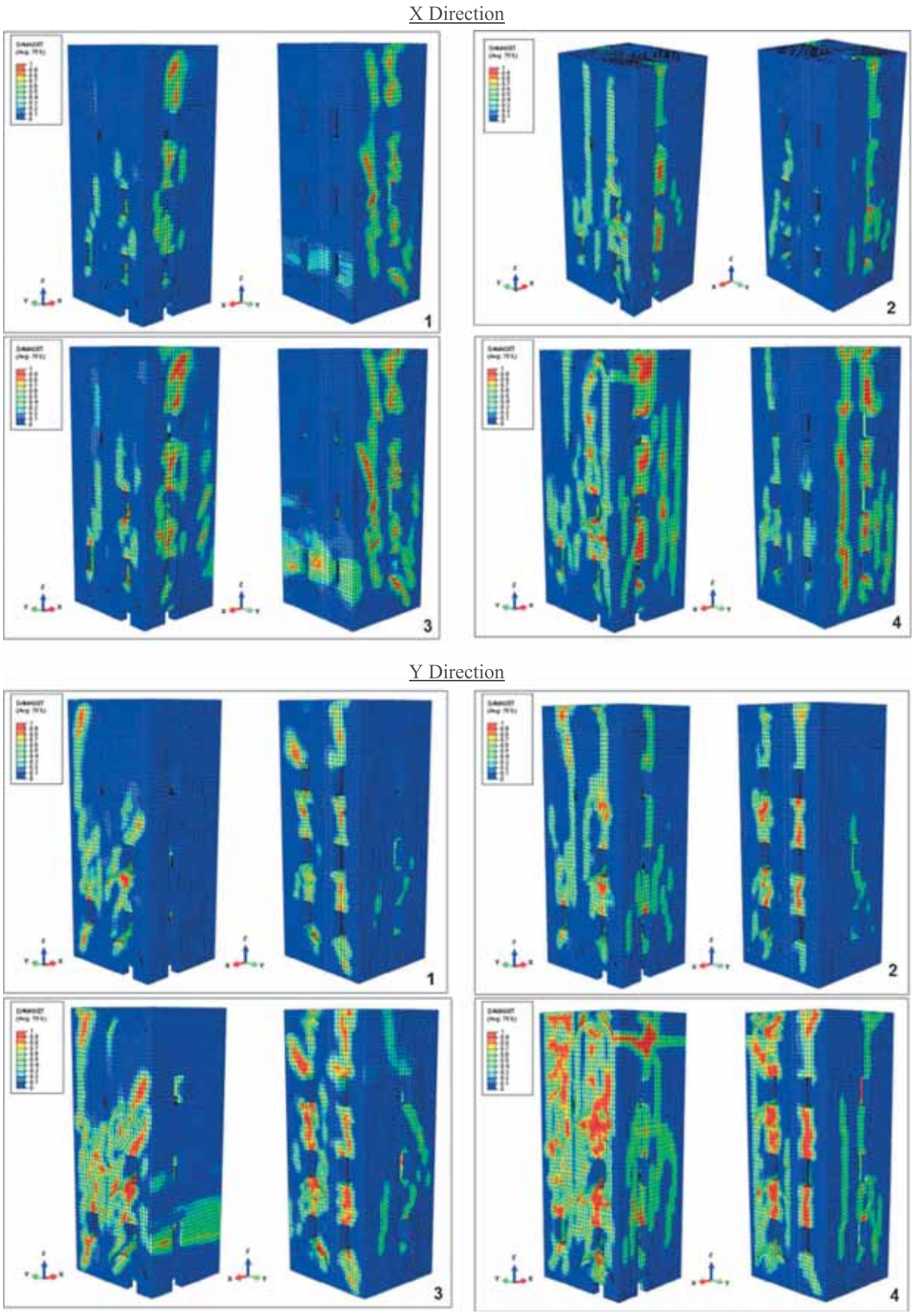

Fig. 34. Tower VIII. Comparison between the damage contour plots obtained through the non-linear static procedure (1 and 3) and the non-linear dynamic analysis (2 and 4). 1 and 2: PGA = 0.1 g. 3 and 4: PGA = 0.2 g.

interesting general agreement is found between the two procedures adopted. Apart from some exceptions due to peculiar geometrical issues (e.g. irregularities and/or leanings), a quite regular trend is observed in dependence of slenderness, cross-section area, openings and walls thickness of the towers.

- The seismic demands obtained by the non-linear static procedure are generally in a good agreement with those obtained by the non-linear dynamic analyses, above all when the check of the structural safety is verified according to the non-linear static procedure. When the check is not satisfied according to the non-linear static procedure, the seismic demand is smaller than the maximum value of the top displacement experienced by the tower during the dynamic simulations. The simplified static approach is not able to capture the inertial effects associated with seismic excitation that can lead to heavy damage and premature collapse of the structure.
- The damage distribution corresponding to the displacement demand in the non-linear static procedure is similar to the one observed at the end of the non-linear dynamic simulations, but the numerical values of damage are smaller. In any case the non-linear static procedure could give a rough indication of the vulnerable parts of the tower, showing the regions of damage concentration.
- The non-linear static procedure may provide reasonable synthetic predictions of the seismic vulnerability of the towers. The two approaches provide similar results in terms of seismic safety assessment, with slightly less conservative predictions for the non-linear static procedure. A comparison between the results obtained by the two approaches shows that the non-linear static procedure is able to assess the structural safety only when local collapse failures are not involved.
- The choice of the control point is a fundamental issue for the application of the non-linear static procedure. The results of the procedure significantly depend on the selection of the control point and show quite large variations with different choices. Therefore, the results obtained by the non-linear static procedure should be evaluated with caution in function of the control point selected for the procedure.

References

[1] Casolo S, Milani G, Uva G, Alessandri C. Comparative seismic vulnerability analysis on ten masonry towers in the coastal Po Valley in Italy. Eng Struct 2013;49:465–90.

[2] Curti E, Lagomarsino S, Podestà S. Dynamic models for the seismic analysis of ancient bell towers. In: Lourenço PB, Roca P, Modena C, Agrawal S, editors. Proc: structural analysis of historical constructions SAHC-2006. New Delhi, India: MacMillan; 2006.

[3] Abruzzese D, Miccoli L, Yuan J. Mechanical behavior of leaning masonry Huzhu Pagoda. J Cultural Heritage 2009;10:480–6.

[4] Carpinteri A, Invernizzi S, Lacidogna G. Numerical assessment of three medieval masonry towers subjected to different loading conditions. Masonry Int 2006;19:65–75.

[5] Riva P, Perotti F, Guidoboni E, Boschi E. Seismic analysis of the Asinelli Tower and earthquakes in Bologna. Soil Dyn Earthq Eng 1998;17:525–50.

[6] Bernardeschi K, Padovani C, Pasquinelli G. Numerical modelling of the structural behaviour of Buti's bell tower. J Cultural Heritage 2004;5:371–8.

[7] Peña F, Lourenço PB, Mendez N, Oliveira D. Numerical models for the seismic assessment of an old masonry tower. Eng Struct 2010;32:1466–78.

[8] Bayraktar A, Sahin A, Özcan M, Yildirim F. Numerical damage assessment of Haghia Sophia bell tower by nonlinear FE modeling. Appl Math Modell 2010;34:92–121.

[9] Milani G, Casolo S, Naliato A, Tralli A. Seismic assessment of a medieval masonry tower in Northern Italy by limit, nonlinear static, and full dynamic analyses. Int J Architect Heritage 2012;6(5):489–524.

[10] Casolo S. A three dimensional model for vulnerability analyses of slender masonry Medieval towers. J Earthq Eng 1998;2(4):487–512.

[11] DM 14/01/2008. Nuove norme tecniche per le costruzioni. Ministero delle Infrastrutture (GU n.29 04/02/2008), Rome, Italy [new technical norms on constructions].

[12] Circolare n° 617 del 2 febbraio 2009. Istruzioni per l'applicazione delle nuove norme tecniche per le costruzioni di cui al decreto ministeriale 14 gennaio 2008 [instructions for the application of the new technical norms on constructions].

[13] DPCM 9/2/2011. Linee guida per la valutazione e la riduzione del rischio sismico del patrimonio culturale con riferimento alle Norme tecniche delle costruzioni di cui al decreto del Ministero delle Infrastrutture e dei trasporti del 14 gennaio 2008 [Italian Guidelines for the evaluation and reduction of the seismic risk of Cultural Heritage, with reference to the Italian norm of constructions].

[14] Comite Europeen de Normalisation. Eurocode 8 EN1998-1 and EN1998-3: design of structures for earthquake resistance. Brussels: CEN; 2004.

[15] ABAQUS®, theory manual, version 6.14.

[16] Valente M. Seismic upgrading strategies for non-ductile plan-wise irregular R/C structures. Procedia Eng 2013;54:539–53.

[17] Valente M. Seismic response of steel buildings with different structural typology. Appl Mech Mater 2013;256–259:2234–9.

[18] Valente M. Seismic strengthening of non-ductile R/C structures using infill wall or ductile steel bracing. Adv Mater Res 2013;602–604:1583–7.

[19] Valente M. Seismic rehabilitation of a three-storey R/C flat-slab prototype structure using different techniques. Appl Mech Mater 2012;193–194:1346–51.

[20] Milani G, Valente M. Comparative pushover and limit analyses on seven masonry churches damaged by the 2012 Emilia-Romagna (Italy) seismic events: possibilities of non-linear finite elements compared with pre-assigned failure mechanisms. Eng Fail Anal 2015;47:129–61.

[21] Milani G, Valente M. Failure analysis of seven masonry churches severely damaged during the 2012 Emilia-Romagna (Italy) earthquake: non-linear dynamic analyses vs conventional static approaches. Eng Fail Anal 2015;54:13–56.

[22] Milani G, Lourenco PB, Tralli A. Homogenised limit analysis of masonry walls. Part I: failure surfaces. Comput Struct 2006;84(3–4):166–80.

[23] Milani G. Simple homogenization model for the non-linear analysis of in-plane loaded masonry walls. Comput Struct 2011;89:1586–601.

[24] Milani G. Simple lower bound limit analysis homogenization model for in- and out-of-plane loaded masonry walls. Constr Build Mater 2011;25:4426–43.

[25] Page AW. The biaxial compressive strength of brick masonry. Proc Inst Civ Engrs, Part 2 1981;71:893–906.

[26] Valente M, Milani G. Seismic assessment of historical masonry towers by means of simplified approaches and standard FEM. Construction and Building Materials 2016;108:74–104. http://dx.doi.org/10.1016/j.conbuildmat.2016.01.025.

[27] Fajfar P. A nonlinear analysis method for performance-based seismic design. Earthq Spectra 2000;16(3):573–92.